

# Late Mesozoic intracontinental deformation and magmatism in the Chinese Tianshan and adjacent areas, Central Asia

Fujun Wang<sup>1</sup>, Meng Luo<sup>1</sup>, Zhiyuan He<sup>2</sup>, Rongfeng Ge<sup>1</sup>, Yuanyuan Cao<sup>3</sup>, Johan De Grave<sup>2</sup>, and Wenbin Zhu<sup>1,†</sup>

<sup>1</sup>State Key Laboratory for Mineral Deposits Research, Institute of Continental Geodynamics, School of Earth Sciences and Engineering, Nanjing University, Nanjing 210023, China

<sup>2</sup>Laboratory for Mineralogy and Petrology, Department of Geology, Ghent University, Krijgslaan 281 S8, 9000 Ghent, Belgium

<sup>3</sup>Xinjiang Institute of Engineering, Urumqi 830023, China

## ABSTRACT

The Tianshan Range–Junggar Basin–Kalamaili Range system represents the southwestern Central Asian Orogenic Belt and is a natural laboratory for studying intracontinental deformation processes. Its current topography is a product of the far-field effects of the Cenozoic India-Asia collision. However, the Mesozoic topographic and tectonic evolution of the Tianshan and Kalamaili Ranges and their impacts on the Junggar Basin remain enigmatic due to the scarcity of data. Here, we present a comprehensive synthesis of sedimentological and geochronological data on these ranges and adjacent basins to reconstruct the intracontinental evolution from the Early Jurassic to the Early Cretaceous. Based on field observations and seismic profile analysis, we identified several unconformities within the late Mesozoic strata in the Tianshan Range and the Junggar Basin. Detrital zircon U-Pb dating results for Lower Jurassic to Lower Cretaceous sandstones of the eastern and southern Junggar Basin, with published paleocurrent data, reveal a complex intracontinental topographic evolution. Moreover, tuffaceous gravels and tuff samples yielded weighted mean zircon  $^{206}\text{Pb}/^{238}\text{U}$  ages of  $156.5 \pm 3.2$  Ma and  $156.3 \pm 2.2$  Ma, respectively, which indicates the presence of contemporary magmatic activity. The deformation and magmatism mentioned above were possibly related to multi-plate convergence in East Asia during the late Mesozoic. This study provides new insights into the late Mesozoic tectonic-magmatic evolution of the Tianshan Range and its adjacent areas.

Fujun Wang  <http://orcid.org/0000-0003-3474-4465>

†Corresponding author: [zwb@nju.edu.cn](mailto:zwb@nju.edu.cn).

## INTRODUCTION

As a main constituent of the vast Central Asian Orogenic Belt, the Tianshan Range is a prominent intracontinental deformation belt in Central Asia. It is widely accepted that the Tianshan Range–Junggar Basin system was initially established in the Paleozoic (Şengör et al., 1993; Xiao et al., 2009; Han et al., 2011; Charvet et al., 2011) and then was reactivated in response to accretionary and collisional events along the Eurasian margin during the Mesozoic (Hendrix et al., 1992; Dumitru et al., 2001; De Grave et al., 2007; Jolivet et al., 2010; Glorie et al., 2011). The tectonic evolution and basin-range coupling relationship between the Tianshan Range and adjacent basins has been widely explored (Hendrix et al., 1992; Greene et al., 2001; Bian et al., 2010; Yang et al., 2013; Tang et al., 2014; Fang et al., 2015; De Pelsmaeker et al., 2018; Nachtergaele et al., 2018). However, many uncertainties remain regarding the Mesozoic tectonic evolution of the regional basin-range dynamics (Jolivet et al., 2013) especially during the Early Jurassic to Early Cretaceous periods. For example, some scholars suggested that the Tianshan Range displayed a positive physiographic feature during the Jurassic (Hendrix et al., 1992; Dumitru et al., 2001; Chen et al., 2011), whereas others argued that the Tianshan Range and Junggar Basin might have been in an extensional tectonic setting due to post-orogenic extension after the Permian collision (Guo et al., 2005; Fang et al., 2006). Regional unconformities at the bases of the Middle Jurassic and Lower Cretaceous sections were identified in the Tianshan Range and Junggar Basin (Vincent and Allen, 2001; Yang et al., 2015a, 2017; this study). Moreover, the extensive occurrence of conglomerates in the Upper Jurassic Kalazha Formation along the Junggar Basin margin further indicates Middle to Late Jurassic tectonic activity. However, these tectonic events are poorly recorded by low-temperature

thermochronological data in the Chinese part of the Tianshan Range (Dumitru et al., 2001; Jolivet et al., 2010, 2013). Contemporaneous cooling is only recorded in the Kyrgyz Tianshan to the west (De Grave et al., 2013; Jepson et al., 2018). Therefore, reliable data on the formation of Jurassic planation surfaces are still quite limited (Jolivet et al., 2013; He et al., 2021a), and they do not reconcile with the Late Jurassic topographic evolution and growth of the range as revealed by sedimentological data (Jolivet et al., 2013). Compared to the basin-range coupling relationship between the Tianshan Range and southern Junggar Basin, the source-to-sink evolution between the Kalamaili Range (Fig. 1) and the eastern Junggar Basin during the Mesozoic is even more unclear due to the scarcity of detrital geochronological data.

The Junggar Basin, located to the north of the Tianshan Range (Fig. 1), preserves a continuous late Paleozoic to Cenozoic sedimentary record with minor hiatuses (Yang et al., 2013; Fang et al., 2015; Xiang et al., 2019). The Jurassic to Quaternary lacustrine to alluvial fan sedimentary sequences are well preserved and widely distributed along the southern and eastern margins of the Junggar Basin (Hendrix, 2000; Fang et al., 2005, 2006, 2015; Charreau et al., 2009; Yang et al., 2013). Based on available detrital geochronological data, late Mesozoic (i.e., Jurassic–Cretaceous) magmatic zircons constitute a significant population of the clastic sediments from the southern and eastern Junggar Basin (Yang et al., 2013; Tang et al., 2014; Fang et al., 2015, 2019; Ji et al., 2018, 2019, 2020). In this regard, the origin of these zircons is an essential issue in understanding late Mesozoic magmatic events in the Tianshan and Kalamaili Ranges. In addition, although paleocurrent data from the late Mesozoic strata suggest that the Tianshan and Kalamaili Ranges were the dominant sediment source areas (Hendrix et al., 1992; Fang et al., 2005, 2015, 2019; Tang et al., 2014; Ji et al., 2018), controversies remain regarding the

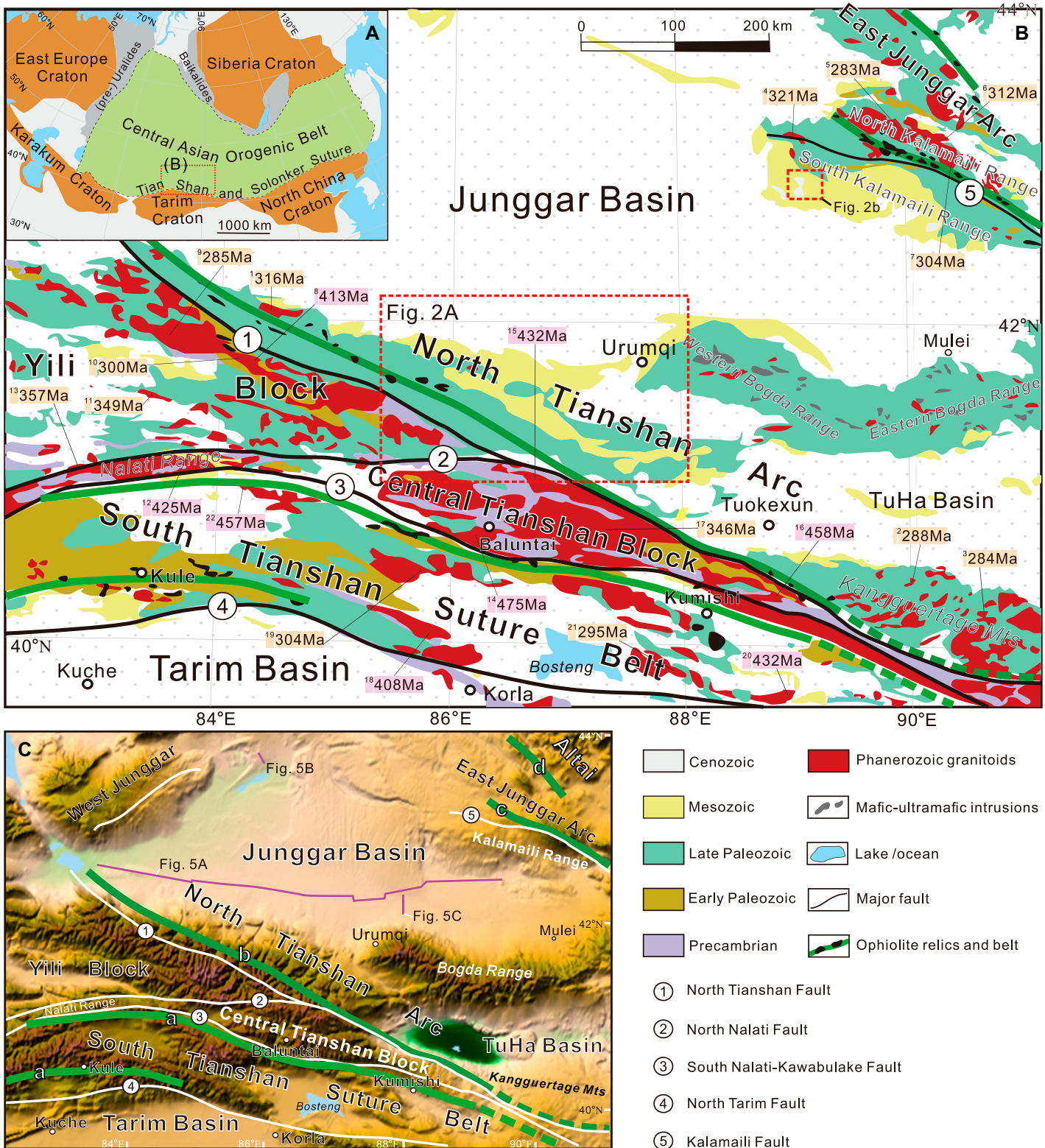


**Figure 1.** (A) Tectonic framework of the Central Asian Orogenic Belt and surrounding regions are after Şengör et al. (1993). (B) Schematic geological map of the Junggar Basin and the Chinese Tianshan Range is after XBGM (2007) and Han and Zhao (2018). (C) Topographic map of the Junggar basin and surrounding mountain belts (from <https://www.ngdc.noaa.gov/mgg/global/>). Names of ophiolite belts: a—South Tianshan ophiolite belt; b—North Tianshan ophiolite belt; c—Kalamaili ophiolite belt; d—Zhaheba-Aermantai ophiolite belt. See Table S1 (see footnote 1) for details on locations and crystallization ages of Paleozoic granitoid intrusions.

source of these zircons due to the poor exposure of late Mesozoic magmatic rocks in these areas.

These uncertainties lead to the need for additional investigation of the late Mesozoic (i.e., Middle Jurassic to Cretaceous) tectono-

magmatic events in the Tianshan area and its surroundings. In this contribution, we present new detrital zircon laser ablation–inductively coupled plasma–mass spectrometry (LA-ICP-MS) U-Pb dating results for Lower Jurassic–Lower

Cretaceous sedimentary rocks in the eastern and southern Junggar Basin (Fig. 2). By combining these data with field observations and seismic profile analyses, we aim to (1) elucidate the late Mesozoic changes in sedimentary provenance

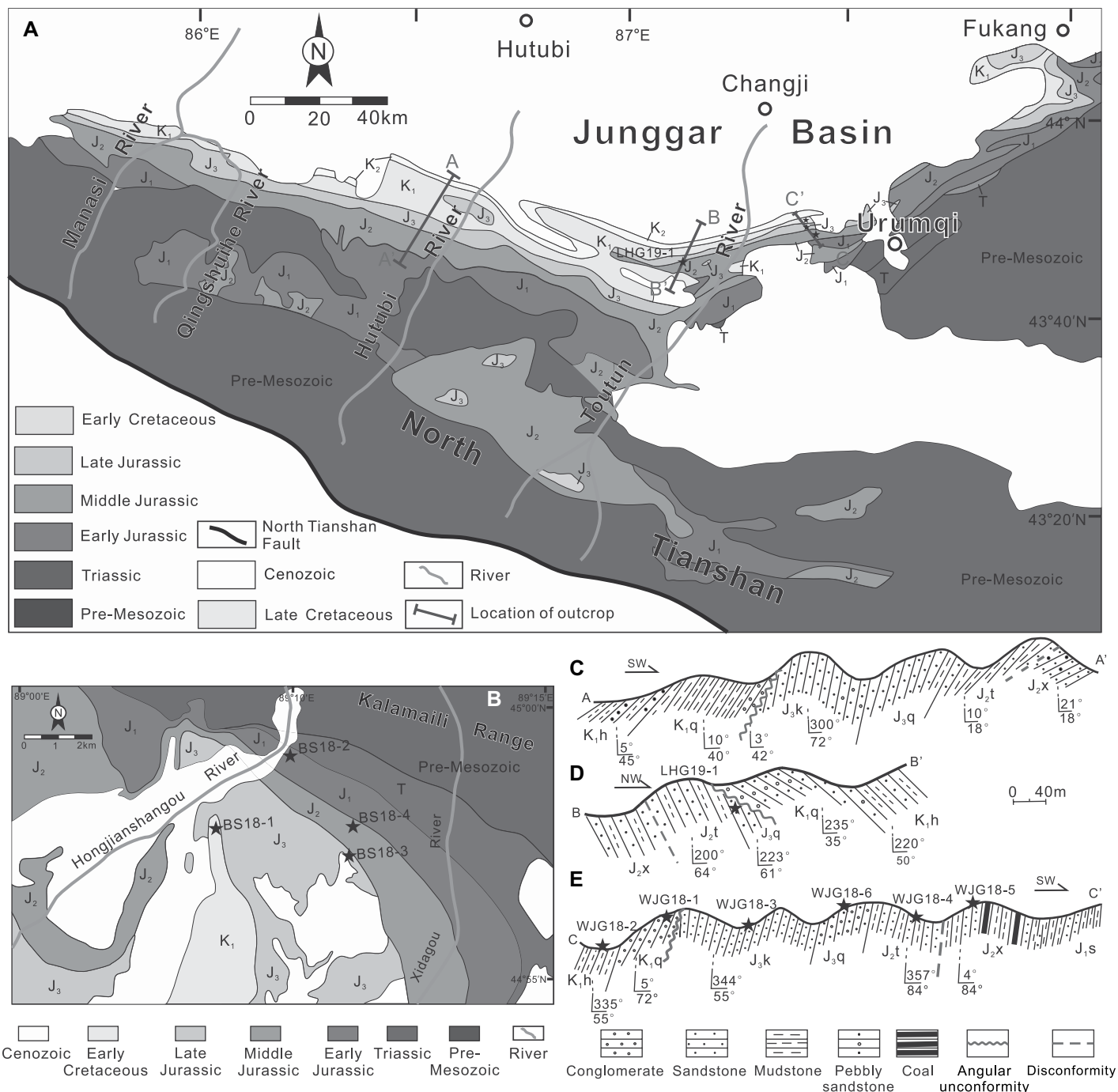


**Figure 2. (A)** Geological map shows the Urumqi area along the southern margin of the Junggar Basin and the North Tianshan Arc (XB-GMR, 2007). **(B)** Geological map shows sampling sites and stratigraphic relations in the eastern Junggar Basin and the Kalamaili Range (XBGMR, 1965). **(C, D, and E)** Cross-sections along the Hutubi (A-A'), Liuhuanggou (B-B'), and Wangjiagou (C-C') areas. J<sub>1</sub>s—Lower Jurassic Sangonghe Formation; J<sub>2</sub>x—Middle Jurassic Xishanyao Formation; J<sub>2</sub>t—Middle Jurassic Toutunhe Formation; J<sub>3</sub>q—Upper Jurassic Qigu Formation; J<sub>3</sub>k—Upper Jurassic Kalazha Formation; K<sub>1</sub>q—Lower Cretaceous Qingshuihe Formation; K<sub>1</sub>h—Lower Cretaceous Hutubi Formation. Sampling locations are indicated by stars.

and the basin-range relationship, (2) identify the source of the late Mesozoic magmatic zircons, and (3) reconstruct the late Mesozoic tectonomagmatic evolution of the Tianshan and Kalamaili Ranges.

## GEOLOGICAL SETTING

### The Tianshan Orogen

The Tianshan Range is a 2500-km-long orogenic belt in Central Asia, and its highest peak is up to 7400 m (Molnar and Tapponnier, 1975). As a major constituent of the southwestern Central Asian Orogenic Belt, it extends from west to east through the Central Asian countries to the Xinjiang province in northwestern China (Gao et al., 1998; Windley et al., 2007; Xiao et al., 2008; Kröner et al., 2014). The Chinese Tianshan Range is geographically divided into the western and eastern segments by the Urumqi-Korla line (Fig. 1; Xiao et al., 2004). It is traditionally subdivided into three tectonic units from north to south by ophiolite belts and major faults that include the North Tianshan Arc, the Yili-Central Tianshan Block, and the South Tianshan Belt (Fig. 1; Gao et al., 1998, 2009; Charvet et al., 2007, 2011; He et al., 2021b).

The South Tianshan Belt is separated from the Tarim Craton to the south by the North Tarim Fault (Fig. 1) and mainly consists of Ordovician to Carboniferous marine sediments with intermittent volcanic sequences and overlying Permian continental clastic rocks, and Mesozoic–Cenozoic clastic successions occur along its southern margin (Gao et al., 1998; Han et al., 2016a; Zhong et al., 2019). Magmatic events in the South Tianshan Belt mainly occurred at ca. 450–380 Ma and ca. 300–270 Ma and were related to the closure of the Paleo-Tianshan Ocean and post-collisional extension (e.g., Konopelko et al., 2009; Huang et al., 2013; Zhao et al., 2015). The Yili–Central Tianshan Block was assembled by the collision between the Yili Block and the Central Tianshan due to the consumption of the intervening Terskey Ocean during the Silurian to Early Devonian (Fig. 1; Gao et al., 2009; Han et al., 2011; Han et al., 2016b). The Yili–Central Tianshan Block is considered to be a micro-continent with a Proterozoic metamorphic basement intruded by various Paleozoic granitic plutons (e.g., Dong et al., 2011; Ma et al., 2014; Wang et al., 2014, 2017; He et al., 2018; Zhu et al., 2019; Su et al., 2021). The North Tianshan Arc traditionally refers to the region between the Yili–Central Tianshan Block and the Junggar Arc and is an accretionary belt composed of Late Carboniferous volcanic-sedimentary rocks and ophiolitic slices (Fig. 1; Wang et al., 2006; Han et al., 2010). This region

predominantly comprises late Paleozoic sedimentary-volcanic strata and magmatic intrusions with no verified Precambrian rocks (Gao et al., 1998). Part of the North Tianshan Arc, the Bogda Range, is dominated by Paleozoic strata covered by Jurassic sediments (Wartes et al., 2002; Chen et al., 2013, 2015). The Bogda Range can be further divided into western and eastern sections (Fig. 1; Ji et al., 2018). The western Bogda Range mainly consists of Late Carboniferous and Early Permian strata (XBGMR, 1993), while the eastern part comprises volcanic-sedimentary rocks of the Ordovician to the Early Carboniferous Qierqusitao Group and the Late Carboniferous Dashitou Group (XBGMR, 1993).

### The Kalamaili Range

The Kalamaili Range is bounded by the Junggar Basin to the south and the Chinese Altai Range to the north (Xiao et al., 2008), and it can further be divided into a southern and northern section along the Kalamaili Fault and ophiolite belt (Fig. 1). The Kalamaili Range is mainly composed of Ordovician to Permian volcanic and siliciclastic rocks, limestones, and cherts (Xu et al., 2015). The South Kalamaili Range mainly consists of the succession of Lower Carboniferous to Permian sedimentary rocks (XBGMR, 1993), while the North Kalamaili Range comprises Ordovician–Carboniferous magmatic rocks (XBGMR, 1993). The ophiolite belt is located along the Kalamaili Fault (Xiao et al., 2014), and recent LA-ICP-MS and secondary ion mass spectrometry (SIMS) zircon U-Pb dating of gabbros and plagiogranites from the ophiolite yielded ages ranging from 417 Ma to 342 Ma (Huang et al., 2012; Xu et al., 2015).

### The Junggar Basin

The Junggar Basin, north of the Tianshan Range, is one of the most prominent walled sedimentary basins in Central Asia (Fig. 1). It began to evolve into an intracontinental basin after the late Paleozoic (Hendrix et al., 1992; Bian et al., 2010; Jolivet et al., 2013; Yang et al., 2013; Zhang et al., 2019). The Mesozoic evolution of this basin, however, remains highly disputed. Some authors proposed that the Mesozoic Junggar Basin was a foreland basin (Hendrix et al., 1992; Hendrix, 2000; Chen et al., 2002), whereas others considered it to be a fault-controlled continental depression in a post-orogenic extensional setting (Allen et al., 1991, 1993; Fang et al., 2006; Jolivet et al., 2010; Yang et al., 2013). The present-day Junggar Basin is an intracontinental foreland basin affected by the distant effects of the Cenozoic India-Asia collision (Avouac et al., 1993; Hendrix et al., 1994; Li et al., 2011; Yang et al., 2013).

## LATE MESOZOIC SEDIMENTATION AND TECTONIC DEFORMATION

### Late Mesozoic Sedimentation

Jurassic to Cretaceous sedimentary sequences are well preserved and exposed in the southern and eastern Junggar Basin (Fig. 2). This section summarizes the observed and published descriptions of lithology, sedimentary facies, and paleocurrent measurements (Fig. 3).

In the southern Junggar Basin, the Lower Jurassic Badaowan Formation ( $J_1b$ ) unconformably overlies the Upper Triassic Xiaoquangou Group ( $T_{3xq}$ ) (Fig. 3). It comprises gray sandstones interbedded with mudstones in the lower part and sandstones and sandy mudstones containing thin coal layers in the upper part (Fang et al., 2005). The coarsening-upward sequence typifies a braided-river delta in the shallow lacustrine environment (Hendrix et al., 1992). The then-prevalent humid climate (Bian et al., 2010) led to coarse-grained deposits with coal streaks. The lake became deeper during the later periods (Fang et al., 2005). In the eastern Junggar Basin, coeval sediments were deposited in a poorly drained alluvial to shallow lacustrine environment (Vincent and Allen, 2001).

The Sangonghe Formation ( $J_1s$ ) in the southern Junggar Basin is dominated by gray-green mudstones and sandstones that bear thin coal streaks and layers (Hendrix et al., 1992; Fang et al., 2005). This sequence corresponds to a braided-river delta to a semi-deep lacustrine environment (Fig. 3), which suggests lake transgression and the southward expansion of the Junggar Basin (Fang et al., 2005). In the eastern Junggar Basin, the sedimentary facies are represented by alluvial plain and lacustrine deposits (Vincent and Allen, 2001).

The Middle Jurassic Xishanyao Formation ( $J_2x$ ) in the southern Junggar Basin comprises gray-green sandstones interbedded with mudstones that are rich in coal layers and streaks, and they can be regarded as shallow-water meandering-river delta to lake swamp deposits (Fig. 3; Fang et al., 2005). This episode is characterized by a warm and wet climate (Chen et al., 2011), and thick coal layers occur in the middle and lower parts (Hendrix et al., 1992; Fang et al., 2005). In the eastern Junggar Basin, the Xishanyao Formation is marked by weaker lacustrine conditions and the recurrence of terrigenous environments (Vincent and Allen, 2001) and thus indicates braided-river delta deposits.

In the southern Junggar Basin, the Middle to Late Jurassic Toutunhe Formation ( $J_{2-3t}$ ) comprises mottled mudstones, sandy mudstones, and sandstones with coal streaks that were deposited in a braided-river sedimentary environment

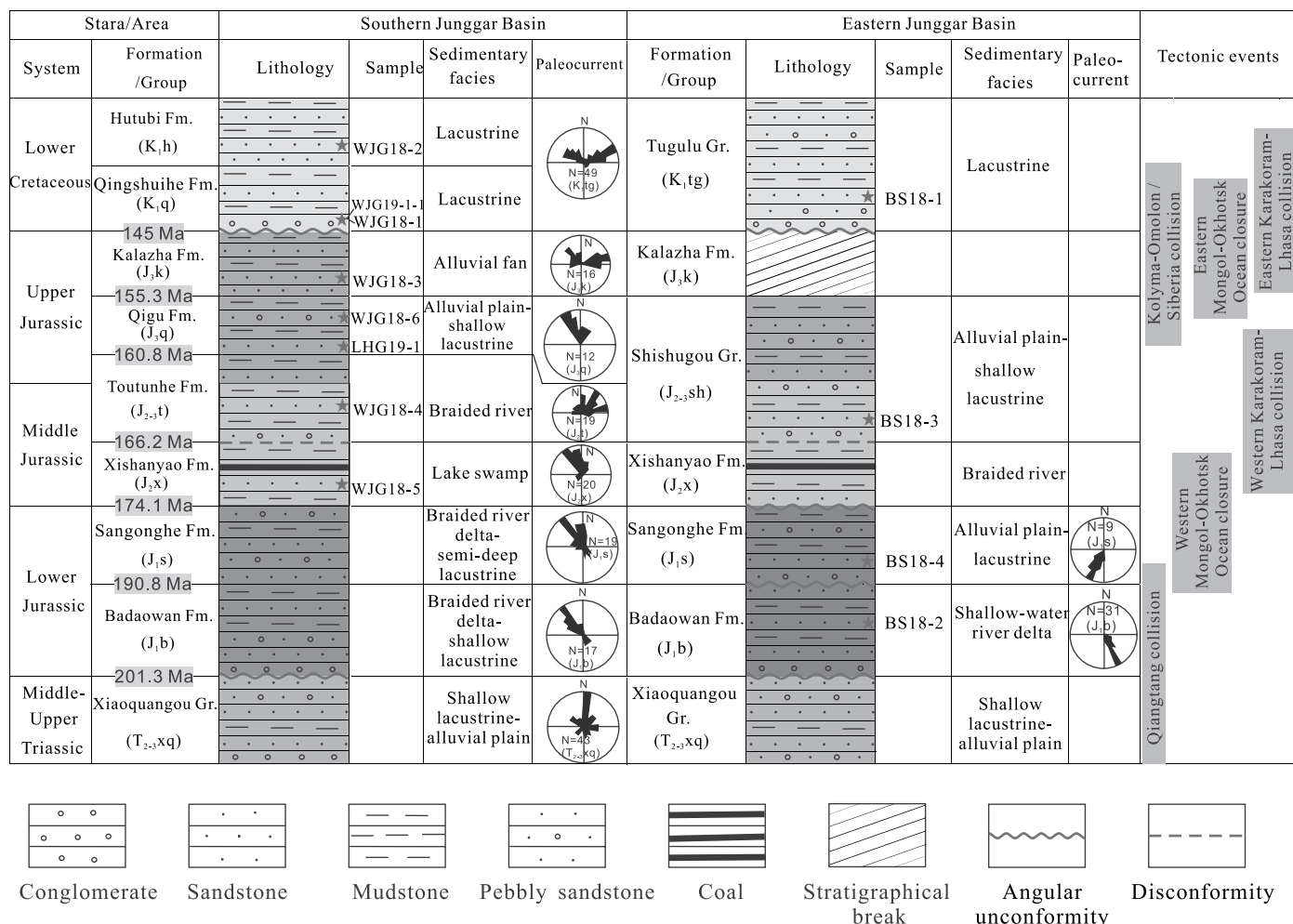


**Figure 3.** Stratigraphy of the Mesozoic strata in the southern and eastern Junggar Basin are shown. Paleocurrent data are from Hendrix et al. (1992) and Fang et al. (2005, 2015). Geologic events are compiled from Yin and Harrison (2000; Qiangtang collision); Zorin (1999; Western Mongol-Okhotsk Ocean closure); Yang et al. (2017; Western Karakoram-Lhasa collision); Oxman (2003; Kolyma-Omolon and Siberia collision); Yang et al. (2015b; Eastern Mongol-Okhotsk Ocean closure); and Yang et al. (2017; Eastern Karakoram-Lhasa collision). Stars represent sampling sites; the locations are shown in Figure 2. Fm.—formation; Gr.—group.

(Hendrix et al., 1992; Fang et al., 2005). The deposition is alternately gray-green and purplish-red, which reflects alternate depositional environments between humid and dry climates (Fig. 3). The Upper Jurassic Qigu Formation ( $J_3q$ ) mainly comprises brown-purple mudstones and sandstones with thinly bedded limestone interlayers at the bottom. The mudstone is restricted in the upper part, which alludes to an ancient arid environment and oxidizing setting (Hendrix et al., 1992; Fang et al., 2005, 2016). The sequence is characteristic of a shallow lacustrine to an alluvial plain environment. The Upper Jurassic Kalazha Formation ( $J_3k$ ) is composed of brown-reddish, thick-bedded conglomerates that represent a sizeable alluvial fan deposit (Fang et al., 2005). The conglomerates unconformably overlie the fine-grained red beds and seem to mark the onset of tectonic uplift of the Tianshan

Range and its adjacent areas (Yang et al., 2013; Fang et al., 2015, 2016).

In the eastern Junggar Basin, the Toutunhe, Qigu, and Kalazha Formations were designated as the Shishugou Group ( $J_{2-3}sh$ ) (Pu et al., 1994; Vincent and Allen, 2001). The sediments of the Shishugou Group are composed of brown-reddish, thick-bedded conglomerates with coarsening-upward sequences deposited in a multiple-phase, alluvial fan environment (Fig. 3; Vincent and Allen, 2001). The Kalazha Formation is absent (Vincent and Allen, 2001).

The Lower Cretaceous Tugulu Group in the southern Junggar Basin consists of the Qingshuihe ( $K_1q$ ) and Hutubi Formations ( $K,h$ ). A regional unconformity was recognized between the Tugulu Group and the underlying Kalazha Formation (Vincent and Allen, 2001). The Tugulu Group contains gray-green mudstones interbed-

ded with sandstones, which indicates a lacustrine environment (Fig. 3; Hendrix et al., 1992; Fang et al., 2005, 2016). In the eastern Junggar Basin, the lowermost Cretaceous strata (equivalent to the Qingshuihe Formation in the southern Junggar Basin) are missing, and the basal Cretaceous unconformity is regionally developed (Vincent and Allen, 2001). In addition, the sedimentary facies boundary that changes from the Upper Jurassic alluvial fan into the Lower Cretaceous lacustrine environment suggests the onset of lake transgression (Vincent and Allen, 2001).

#### Late Mesozoic Tectonic Deformation

Several unconformities are identified in the Tianshan Range and its adjacent areas within the late Mesozoic sequences. The Cretaceous basal unconformities are regionally developed and

were observed at several sections in the Tianshan Range and its adjacent basins (Yang et al., 2015a). In the Tianshan Range, the Lower Cretaceous Tugulu Group overlies the Middle Jurassic Toutunhe Formation, while the Upper Jurassic Qigu and Kalazha Formations are absent (Yang et al., 2017). In the Tarim, Junggar, and Turpan-Hami basins, the Upper Jurassic strata are only locally observed. Meanwhile, conglomerates are widely distributed at the base of the Lower Cretaceous strata in these basins and delineate an angular unconformity. Our field observations in the southern Junggar Basin also indicate the occurrence of this widespread unconformity surface (Figs. 4A–4C). For example, in the Hutubi section, the occurrence of the Lower Cretaceous Qingshuihe Formation ( $K_1q$ ) conglomerate is  $10^\circ \angle 40^\circ$ , whereas that of the underlying Upper Jurassic Kalazha Formation ( $J_3K$ ) sandstone is  $300^\circ \angle 72^\circ$  (Fig. 4A). The same unconformity was examined in the Liuhuanggou (Fig. 4B) and Wangjiagou sections (Fig. 4C). In the former section, the orientation and dip of the conglomerate in the Lower Cretaceous Qingshuihe Formation is  $340^\circ \angle 68^\circ$ , and the sandstone in the Upper Jurassic Kalazha Formation shows values of  $355^\circ \angle 78^\circ$ , which indicates an angular unconformity (Fig. 4B). In the latter section, the occurrence of the strata above the unconformity is  $335^\circ \angle 55^\circ$  and the strata under the unconformity exhibit  $5^\circ \angle 72^\circ$  (Fig. 4C). These regional angular unconformities indicate that Late Jurassic to Early Cretaceous tectonic events have exerted a broad effect on the Tianshan Range and Junggar Basin.

Prior to the Late Jurassic to Early Cretaceous deformation, the Tianshan Range and Junggar Basin also underwent intense deformation during the Middle Jurassic (Yang et al., 2015a). A local disconformity between the Middle Jurassic Toutunhe Formation and the underlying Xishanyao Formation was found along several margins of the Junggar Basin (Figs. 4D–4F; Vincent and Allen, 2001; He et al., 2007; Yang et al., 2015a, 2017). In the Hutubi section, a conglomerate layer interbedded with sandstone with cross-bedding was observed in the lower part of the Toutunhe Formation. It changes upward into red and green sandstone and mudstone (Fig. 4D). The gravels at the bottom of the Toutunhe Formation display well-rounded clasts with high maturity. The upper part of the underlying Xishanyao Formation consists of a series of gray (non-pebbled) quartz sandstones with cross-bedding. The top of the quartz sandstone layer is convex and uneven, representing an unconformity and a depositional gap. The dip angles of the strata above and below the unconformity are similar (Fig. 4D), indicating a disconformity. Similar disconformities were also identified in

the Liuhuanggou (Fig. 4E) and Wangjiagou sections (Fig. 4F) near Urumqi. In the eastern Junggar Basin, disconformity planes also occur at the base of the Xishanyao and Shishugou Formations. Vincent and Allen (2001) suggested that the generation of these unconformities resulted from episodic uplift in the Kalamaili Range.

Seismic images show clear Lower Cretaceous base unconformities at the margin and center of the Junggar Basin (Fig. 5; Yang et al., 2015a; Wang et al., 2018a). Below the unconformity, the Upper and Middle Jurassic strata were truncated, and the Upper Jurassic strata are absent within the basin. The dip angles between Jurassic and Lower Cretaceous strata are different, which indicates an angular unconformity (Fig. 5) due to intense deformation events. These events also led to folding in the central depression (Fig. 5). The Jurassic strata under the unconformity dip gently in the northwestern and central sections (Figs. 5A–5B) and steeply in the southeastern regions (Fig. 5C), which indicates that local deformation in the eastern and southern Junggar Basin was more intensive than that in the northwestern and central areas of the basin. This Lower Cretaceous unconformity is also observed in the Tianshan Range (Yang et al., 2015b, 2017) and extends westward to Kazakhstan (Jolivet et al., 2013), which probably indicates a widespread regional tectonic event. Also, in the Tianshan Range, the lack of the Upper Jurassic Qigu and Kalazha Formations implies that this tectonic event may have initiated after the depositional period of the Toutunhe Formation. The Toutunhe Formation was also locally truncated in the Junggar Basin (Fig. 5; Yang et al., 2015b). Seismic profiles through the Junggar Basin show that a fold nappe formed on the hanging wall of a thrust fault during the Late Jurassic (Fig. 5), which led to denudation of the Upper Jurassic strata on the top of the fold. Corresponding growth strata are widely distributed at the basin margins and the center. They are visible in the seismic profiles of the late Middle Jurassic Toutunhe Formation and the Upper Jurassic Qigu and Kalazha Formations (Figs. 5B–5C; Wang et al., 2018a). These lines of evidence show that both the Tianshan and its adjacent areas experienced regional intracontinental deformation from the Middle Jurassic to the Early Cretaceous.

## DETrital ZIRCON LA-ICP-MS U-Pb GEOCHRONOLOGY

### Sandstones and Conglomerates

A total of 10 sandstone samples from the Lower Jurassic to Lower Cretaceous strata in the eastern and southern Junggar Basin were collected for detrital zircon LA-ICP-MS U-Pb

dating. More than 100 zircon grains were picked from each sample. Cathodoluminescence (CL) images of typical zircon grains are presented in Figure 6. Detailed descriptions of the analytical methods used here can be found in Supplemental Material Tables S1–S3<sup>1</sup>. The results are listed in Table S2. Zircon ages younger than 1000 Ma are based on  $^{206}\text{Pb}/^{238}\text{U}$  ratios, whereas ages older than 1000 Ma are based on  $^{207}\text{Pb}/^{206}\text{Pb}$  ratios. Ages with a discordance degree of <10% are used in the discussion (Fig. 7). The detrital zircon U-Pb age groups and the corresponding statistical data are shown in Table 1. The ages obtained from the 10 samples range from 3160 Ma to 125 Ma and can be divided into four groups: 3160–542 Ma (Precambrian), 538–382 Ma (early Paleozoic), 378–253 Ma (late Paleozoic), and 251–125 Ma (Mesozoic) (Fig. 8; Table 1). Most Mesozoic and Paleozoic zircons show well-developed oscillatory zoning (Fig. 6) and higher Th/U ratios (>0.4) (Table S2), which suggests a magmatic origin. Most of the Precambrian zircons are interpreted to reflect a magmatic origin, and very few can be regarded as metamorphic zircons due to their faint internal zoning or inherited cores (Fig. 6; Hoskin and Black, 2000; Corfu et al., 2003).

### Samples from the Eastern Junggar Basin

Sample BS18-2 was collected from a gray, coarse-grained sandstone in the middle part of the Lower Jurassic Badaowan Formation. Late Paleozoic zircons from this sample range from 253 Ma to 366 Ma in age, with two prominent peaks at 327 Ma and 287 Ma (Fig. 8A; Table 1). The second population is represented by early Paleozoic zircons that range from 515 Ma to 429 Ma (13%), with one subordinate peak at 456 Ma. There are also a few early Mesozoic zircon grains (250–194 Ma). These zircons generally are elongated euhedral crystals with clear oscillatory zoning (Fig. 6A) and have high Th/U ratios of 0.40–2.92 (Table S2), which indicates a magmatic origin. An additional four zircons display Neoproterozoic ages (955–894 Ma) (Fig. 6A). Sample BS18-4 was collected from the bottom of the Lower Jurassic Sangonghe Formation. The age spectrum of this sample is similar to that of sample BS18-2 except for a noticeable increase in early Paleozoic zircons. Most zircons show high Th/U ratios that range

<sup>1</sup>Supplemental Material. Supplementary text: Analytical methods. Table S1: Location and crystallization ages of Paleozoic granitoid intrusions. Table S2: LA-ICP-MS zircon U-Pb dating results of detrital samples. Table S3: LA-ICP-MS zircon U-Pb dating results of gravel and tuff samples. Please visit <https://doi.org/10.1130/GSAB.S.19027355> to access the supplemental material, and contact [editing@geosociety.org](mailto:editing@geosociety.org) with any questions.

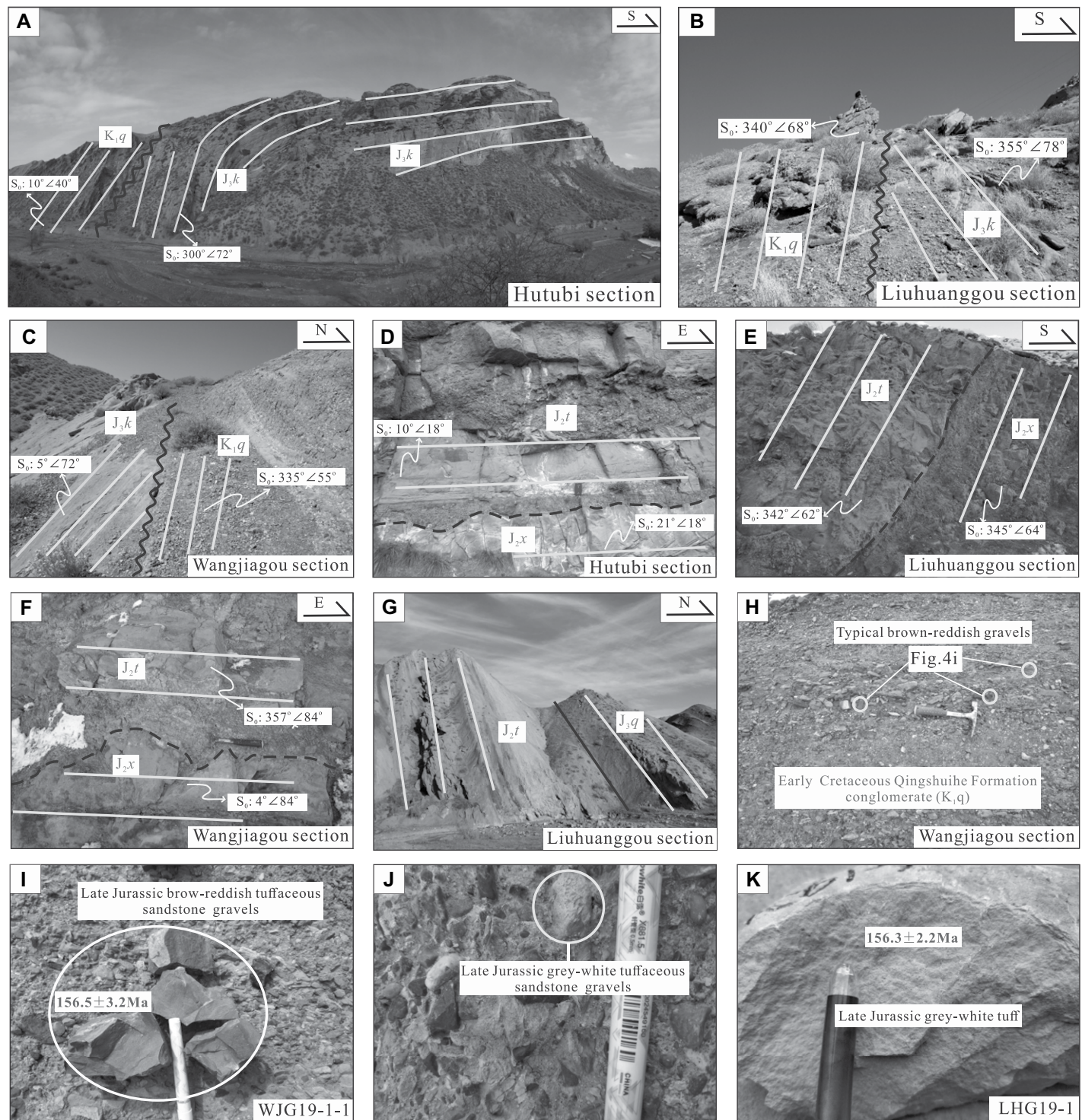


**Figure 4.** Field photographs are from the southeastern Junggar Basin. (A–C) Angular unconformity between the Qingshuuhe Formation ( $K_1q$ ) and the Kalazha Formation ( $J_3k$ ) in (A) the Hutubi section, (B) Liuhuanggou section, and (C) Wangjiagou section. (D–F) Disconformity between the Toutunhe Formation ( $J_{2-3}t$ ) and the Xishanyao Formation ( $J_2x$ ) in (D) the Hutubi section, (E) Liuhuanggou section, and (F) Wangjiagou section. (G) Contact between the Qigu and Toutunhe Formations. (H–J) Typical gravels from the Qingshuuhe Formation ( $K_1q$ ) conglomerate. (K) Tuff from the Upper Jurassic Qigu Formation ( $J_3q$ ).

from 0.40 to 2.38 (Table S2) and well-developed oscillatory zoning (Fig. 6B), which suggests a dominant origin from magmatic rocks.

Sample BS18-3 was sampled from the Middle–Upper Jurassic Shishugou Group, and 45% concordant analyses yielded late Pale-

zoic ages (362–256 Ma with a peak at 330 Ma) (Table 1). In addition, ~14% of the dated zircons have Early to Middle Jurassic U-Pb ages

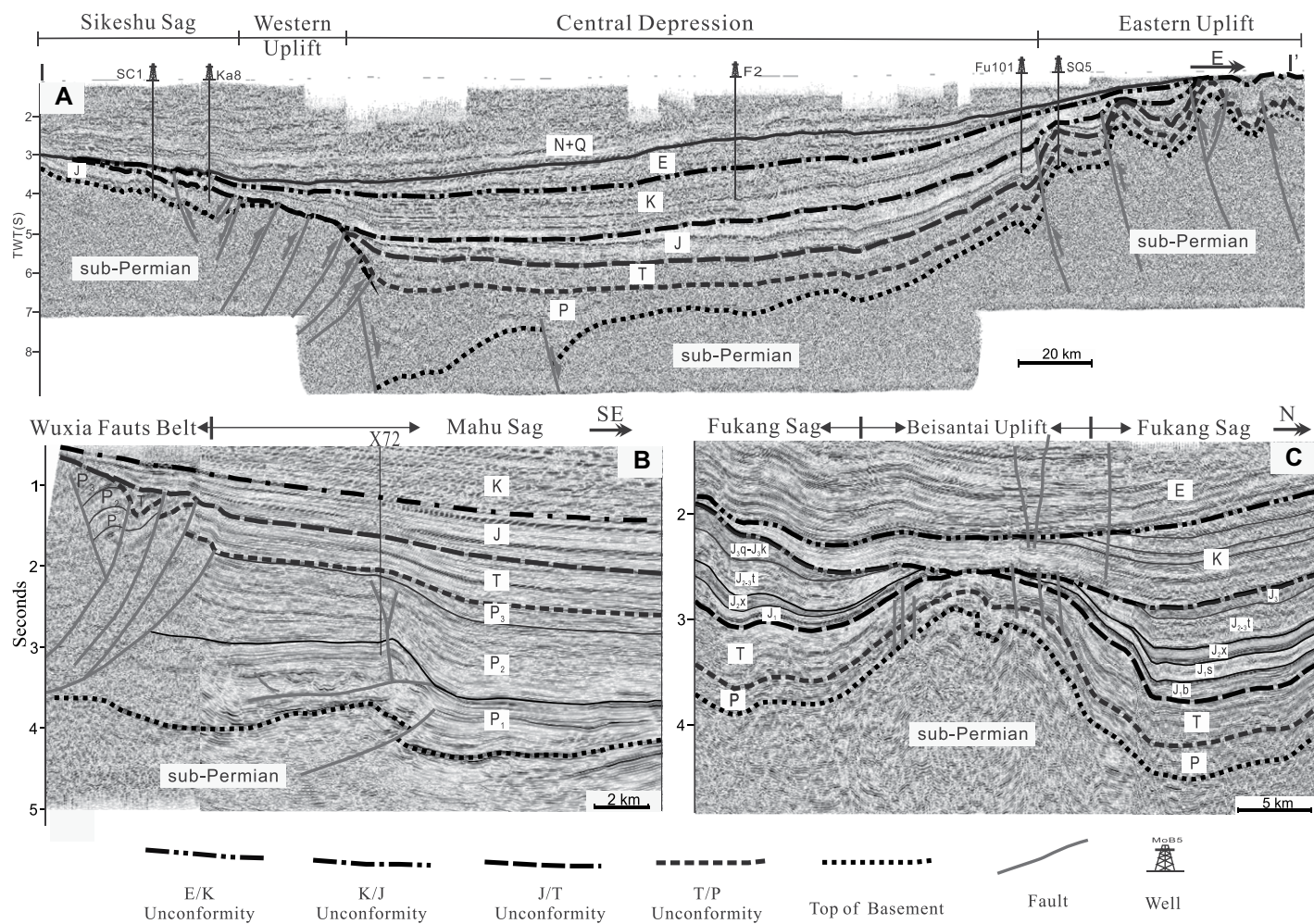


**Figure 5. Seismic profiles through (A) the Junggar Basin, (B) the Wuxia Fault Belt and Mahu sag basin in northwestern Junggar, and (C) the Fukang sag basin and the Beisantai Uplift in southeastern Junggar. The original seismic profiles are from Wang et al. (2018a). The location is shown in Figure 1B. P—Permian; P<sub>1</sub>—Lower Permian; P<sub>2</sub>—Middle Permian; P<sub>3</sub>—Upper Permian; T—Triassic; J—Jurassic; J<sub>1</sub>—Lower Jurassic; J<sub>2</sub>—Middle Jurassic; J<sub>3</sub>—Upper Jurassic; K—Cretaceous; E—Paleogene; N—Neogene; Q—Quaternary.**

that range from 198 Ma to 158 Ma, with a young age peak of 173 Ma (Fig. 8C; Table 1). These zircons are euhedral in shape with well-developed oscillatory zoning (Fig. 6C) and high Th/U ratios (Table S2). Thus, they are interpreted to be of magmatic origin, which indicates the presence of Jurassic magmatic components in the source.

Sample BS18-1 was collected from the Lower Cretaceous Tugulu Group. Compared with the Jurassic samples, the proportion of Jurassic-age zircons in this sample (180–148 Ma with an age peak of 161 Ma) significantly increases from 14% to 47% (Fig. 8D; Table 1). In contrast, the late Paleozoic zircon population (371–258 Ma with an age peak at 309 Ma) decreases to 36%. Based on their well-developed oscillatory zoning (Fig. 6D) and high Th/U ratios (0.29–3.78), almost all of the zircons in this sample have a magmatic origin (Table S2).

#### Samples from the Southern Junggar Basin

Sample WJG18-5 was taken from a gray-green, coarse-grained sandstone at the base of the Middle Jurassic Xishanyao Formation. Abundant late Paleozoic zircons exhibit U-Pb ages ranging from 373 Ma to 271 Ma, with two prominent peaks at 367 Ma and 305 Ma (Fig. 8E; Table 1). In addition, early Paleozoic zircon grains are also a key component (~39%), with a peak age at 416 Ma. The majority of the zircons from this sample are magmatic in origin, as shown by their high Th/U ratios ranging from 0.24 to 1.74 (Table S2) and clear oscillatory zoning patterns (Fig. 6E).

Sample WJG18-4 is from red, coarse-grained sandstone and was collected from the Middle Jurassic Toutunhe Formation. It differs from the previous samples by the first appearance of a group of Middle–Late Jurassic zircons (~36%), ranging in age from 175 Ma to 151 Ma, with a

prominent peak at 161 Ma (Fig. 8F; Table 1). The late Paleozoic zircons are another significant component in this sample (~34%), with a prominent peak at 295 Ma. The proportion of early Paleozoic zircon significantly decreases to 19% compared to the previous sample. Almost all of these zircons are attributed to magmatic origins according to their well-developed oscillatory zoning (Fig. 6F) and high Th/U ratios (Table S2).

Samples WJG18-6 and WJG18-3 are from the Upper Jurassic Qigu and Kalazha Formations, respectively. Similar to sample WJG18-4, the Jurassic zircons are a dominant group, with ages ranging from 197 Ma to 155 Ma (with peaks at 169 Ma and 165 Ma, respectively) (Figs. 8G–8H; Table 1). Compared with the Middle Jurassic samples, the proportion of the early Paleozoic zircons decreases significantly. Almost all late Mesozoic and Paleozoic zircons display well-developed oscillatory zoning (Figs. 6G–6H) and

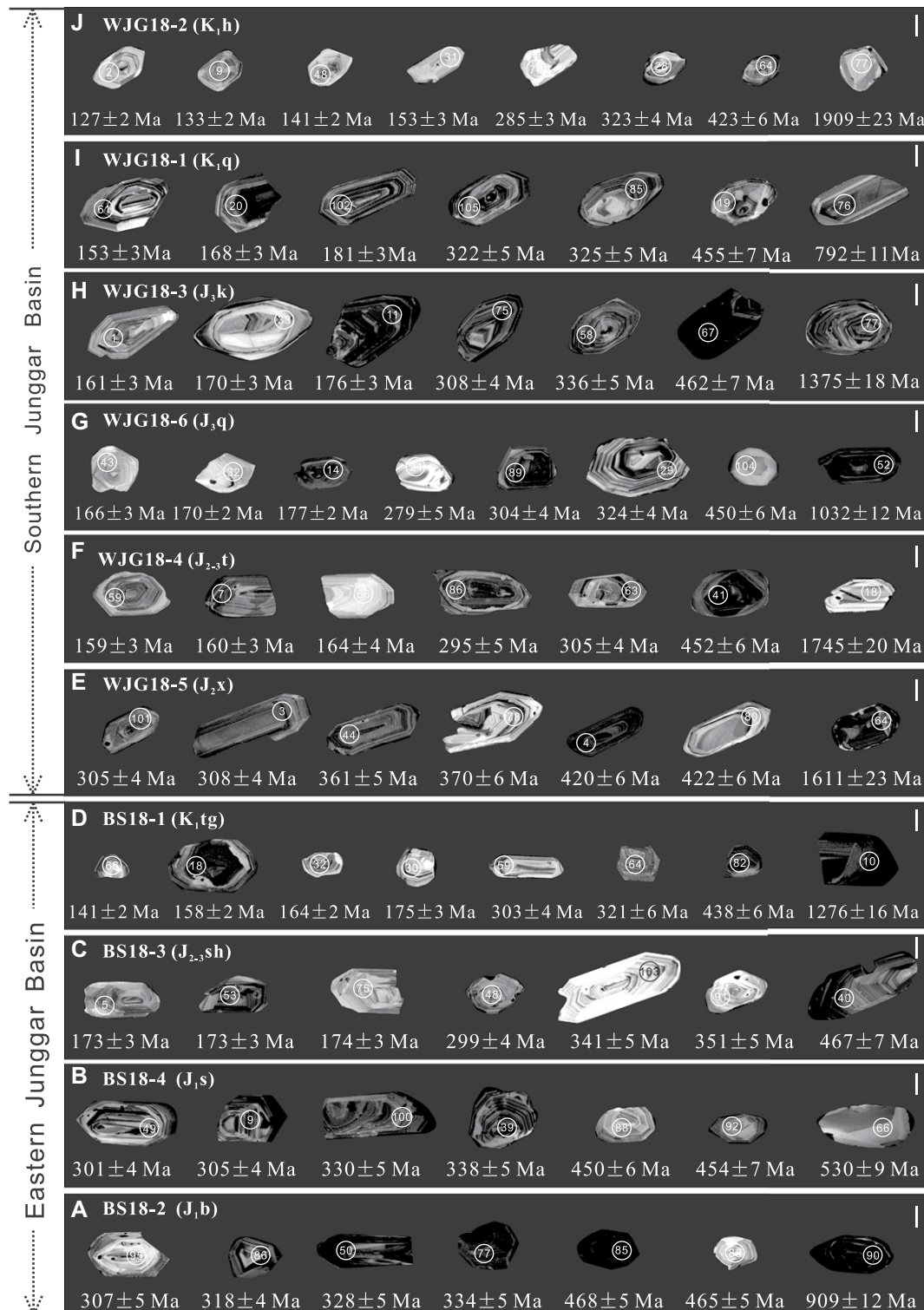


**Figure 6.** Cathodoluminescence (CL) images of representative detrital zircons from the Lower Jurassic to Upper Cretaceous samples in (A–D) the eastern Junggar Basin and (E–J) the southern Junggar Basin are shown. Circles indicate positions of laser spots for age analyses. The analytical numbers and apparent ages are indicated. Scale bar = 24  $\mu$ m.

have high Th/U ratios (Table S2), which is suggestive of a magmatic origin.

Sample WJG18-1 was collected from a gray conglomerate in the Lower Cretaceous Qingshuihe Formation. This sample is dominated by late Paleozoic zircons that range in age from

377 Ma to 254 Ma (~51%), with a prominent peak at 321 Ma. The second population is formed by early Paleozoic zircons (531–390 Ma, a peak at 454 Ma) (Fig. 8I; Table 1). Abundant Jurassic zircons yield ages from 200 Ma to 153 Ma with a peak at 169 Ma (11%). These zircons are

of magmatic origin as indicated by their elongated euhedral crystal habit with clear oscillatory zoning (Fig. 6I) and high Th/U ratios that range from 0.25 to 3.63 (Table S2). Unlike other samples, abundant Precambrian zircons from the age interval 2789–542 Ma account for 17%.

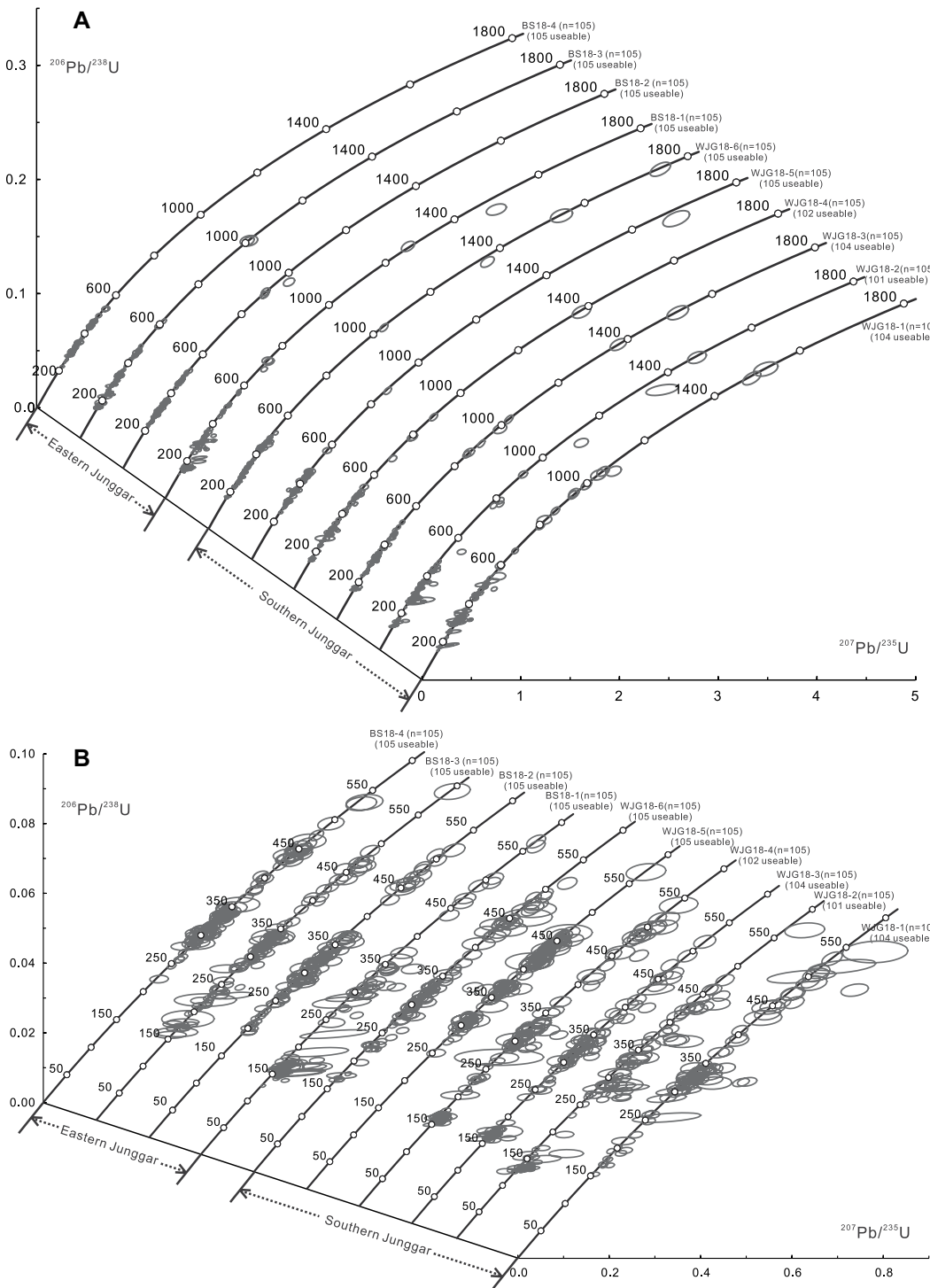


**Figure 7.** U-Pb Concordia plots for detrital zircons of the Lower Jurassic to Upper Cretaceous samples in the southern and eastern Junggar Basin are shown. (A) <1800 Ma grains. (B) <600 Ma grains.

Sample WJG18-2 is from red, fine-grained sandstone in the Lower Cretaceous Hutubi Formation. It differs from all previous samples by the first appearance of abundant Early Cretaceous zircons that range in age from 143 Ma to 125 Ma (~20%), with a prominent peak at 131 Ma, which indicates the presence of Cretaceous source rocks (Fig. 8J; Table 1). Late Paleozoic zircons (375–258 Ma) are still significant

in this sample and account for 45% of the total (Table 1). These zircons are interpreted as having a magmatic origin based on their well-developed oscillatory zoning (Fig. 6J) and high Th/U ratios.

#### Tuffaceous Gravels and Tuff Samples

Zircon U-Pb dating results for tuffaceous gravels and tuff samples are presented in

Table S3, and the ages are plotted on Concordia diagrams (Fig. 9). Most of the zircons from the gravel and tuff samples are euhedral to subhedral in shape, with length/width ratios that range from 2:1 to 4:1. They show clear oscillatory zonation (Fig. 9) and have relatively high Th/U ratios that range from 0.44 to 2.96 (Table S3), which indicates an igneous origin.

TABLE 1. DETRITAL ZIRCON U-PB AGE GROUPS OF THE 10 SAMPLES

Sample no. and stratigraphic age	Precambrian zircons (542–3149 Ma)	Paleozoic zircons (253–538 Ma)		Mesozoic zircons (125–251 Ma)		
		Early Paleozoic (382–538 Ma)	Late Paleozoic (253–380 Ma)	Triassic (201–251 Ma)	Jurassic (148–200 Ma)	Cretaceous (125–143 Ma)
<u>Lower Cretaceous samples</u>						
WJG18-2 (K <sub>1</sub> h) 101	762–1934 8%	382–527 (425) 17%	258–375 (286) 45%	230–251 2%	149–195 (168) 8%	125–143 (131) 20%
WJG18-1 (K <sub>1</sub> g) 104	542–2801 17%	390–531 (454) 19%	254–377 (321) 51%	212–248 2%	153–200 (169) 11%	
BS18-1 (K <sub>1</sub> tg) 105	558–1968 8%	438–502 6%	258–371 (309) 36%	218–244 2%	148–180 (161) 47%	138 1%
<u>Upper Jurassic samples</u>						
WJG18-3 (J <sub>2</sub> k) 104	857–2223 8%	386–516 (452) 13%	261–379 (318) 35%	236–251 4%	155–189 (165) 30%	
WJG18-6 (J <sub>2</sub> q) 105	1032–1758 4%	387–510 (442) 27%	254–373 (301) 53%	221–242 10%	166–197 (169) 6%	
<u>Middle Jurassic samples</u>						
BS18-3 (J <sub>2</sub> sh) 105	590–2584 7%	384–487 (466) 17%	256–362 (330) 45%	204–249 (233) 17%	158–198 (173) 14%	
WJG18-4 (J <sub>2</sub> t) 102	681–2505 6%	398–538 (454) 18%	254–370 (295) 34%	203–235 8%	151–175 (161) 36%	
WJG18-5 (J <sub>2</sub> x) 105	570–3149 4%	387–464 (416) 39%	271–373 (305) 56%	250 1%		
<u>Lower Jurassic samples</u>						
BS18-4 (J <sub>1</sub> s) 105		391–530 (445) 26%	257–380 (337) 72%	222–245 2%		
BS18-2 (J <sub>1</sub> b) 105	894–1105 4%	429–515 (456) 13%	253–366 (327) 67%	201–250 13%	194–199 3%	

Twenty-five grains from the tuffaceous gravels (sample WJG19-1-1) were chosen for U-Pb dating, and 24 effective data points were obtained. The zircons have variable Th (88.1–856 ppm) and U (94.4–1196 ppm) contents with high Th/U ratios (0.52–2.96). On the Concordia diagram (Fig. 9A), four spots yielded a weighted mean  $^{206}\text{Pb}/^{238}\text{U}$  age of  $156.5 \pm 3.2$  Ma ( $1\sigma$ , MSWD = 1.18). This age is taken to represent the time of volcanic activity associated with the tuff formation. The other 20 analyses show  $^{206}\text{Pb}/^{238}\text{U}$  ages of  $>247$  Ma and are probably inherited zircons. Most of these zircons are late Paleozoic in age (347–284 Ma).

Twenty-four analyses from sample LHG19-1 (tuff) were conducted on 24 grains. U (127.2–2747 ppm) and Th (154.2–3050 ppm) contents are highly variable, with Th/U ratios of 0.45–2.72. Nine analyses defined an age population and had a weighted mean  $^{206}\text{Pb}/^{238}\text{U}$  age of  $156.3 \pm 2.2$  Ma ( $1\sigma$ , MSWD = 1.08) (Fig. 9B). We interpreted this age as the time of volcanic activity related to the tuff formation. The other 15 analyses show  $^{206}\text{Pb}/^{238}\text{U}$  ages of  $>279$  Ma, which suggests these grains are probably inherited zircons. These are dominated by the late Paleozoic zircons (342–279 Ma).

## DISCUSSION

### Variation of Provenance

Paleocurrent measurements from the late Mesozoic strata in the southern Junggar Basin indicated that the Tianshan Range was the dominant provenance area during this time (Hendrix et al., 1992; Fang et al., 2005, 2015). However, southward-flowing paleocurrents from the Lower Jurassic to Lower Cretaceous strata in the eastern Junggar Basin alternatively suggested that the Kalamaili Range was the dominant source area (Hendrix et al., 1992; Vincent and Allen, 2001). The zircon U-Pb age spectra of

detrital samples show a significant multimodal distribution, which implies a diverse provenance and the possible joining of other sources during the Early Jurassic–Early Cretaceous.

### Provenance Changes of the Eastern Junggar Basin

The U-Pb age pattern of the detrital zircons from the Lower Jurassic Badaowan Formation (sample BS18-2) shows similarities to those of the Sangonghe Formation (sample BS18-4). The latter is characterized by a significant multimodal distribution with two dominant early Carboniferous to Early Permian age peaks and a minor Ordovician age peak (Figs. 8A–8B). The Kalamaili Range is dominated by Ordovician to Permian volcanic and siliciclastic rocks (Xiao et al., 2006). The succession of Lower Carboniferous–Permian sedimentary rocks is well developed in the South Kalamaili Range (XBGMR, 1993). The early Paleozoic arc magmatic rocks are primarily distributed in the Yemaquan area along the North Kalamaili Range (Li et al., 2009). Combined with southward-flowing paleocurrents in the eastern Junggar Basin (Fang et al., 2005), these late Paleozoic zircons are thus mainly derived from the late Paleozoic magmatic belt of the South Kalamaili Range, while early Paleozoic zircons are derived from the North Kalamaili Range (Fig. 10A). Compared with the Badaowan Formation, the proportion of early Paleozoic zircons (peak age at 445 Ma) in the Sangonghe Formation slightly increased (Figs. 8A–8B), which indicates the erosion of the older sedimentary sources (Fig. 10A). Proterozoic ages are nearly absent. Most scholars believe that solid evidence for Precambrian rocks is still lacking in the eastern Junggar Basin and Kalamaili Range (Xiao et al., 2004; Long et al., 2012; Han and Zhao, 2018). However, Xu et al. (2015) argued that a Precambrian basement exists in this region due to the discovery of ca. 2.5 Ga and ca. 1.9 Ga gneiss and quartz-

ite enclaves in a dioritic dike in the South Kalamaili Range.

There is a dramatic change in the age spectrum of the Upper–Middle Jurassic Shishugou Group (sample BS18-3), with the first appearance of Jurassic magmatic zircons (peak age at 173 Ma) (Fig. 8C), which indicates syn-depositional magmatic sources. Pu et al. (1994) also found Late Jurassic tuffs in the lower part of the Qigu Formation in the Cainan section near the Kalamaili area. Their occurrence suggests that magmatic activity probably took place in the Kalamaili Range during the early depositional phase of the Shishugou Group (Fig. 10C). The other two sources of zircons again correspond to the late Paleozoic magmatic rocks of the South Kalamaili Range (peak age at 330 Ma) and the early Paleozoic magmatic rocks of the North Kalamaili Range (peak age at 466 Ma), respectively (Fig. 10D). The older-age zircons may be derived from recycling of the underlying cover deposited in the South Kalamaili Range.

The age population pattern of the Lower Cretaceous Tugulu Group (sample BS18-1) still yields Middle to Late Jurassic magmatic zircons (peak age at 161 Ma) (Fig. 8D), which reflects recycling from the underlying Middle–Late Jurassic sedimentary series (Fig. 10E). Compared with sample BS18-3, the proportion of the Paleozoic age population in this sample dropped markedly, which indicates that the sedimentary contribution of the Paleozoic magmatic rocks from the Kalamaili Range further decreased. The sharp facies boundary from the Upper Jurassic alluvial fan to the Lower Cretaceous lacustrine environment (Yang et al., 2013), together with potential recycling of the Jurassic series, suggest the onset of a new lake transgression (Fig. 10E). This event may reflect renewed active erosion during the Early Cretaceous in accordance with the ca. 130 Ma apparent apatite fission-track ages obtained in the Kalamaili Range (Li et al., 2014; He et al., 2022).

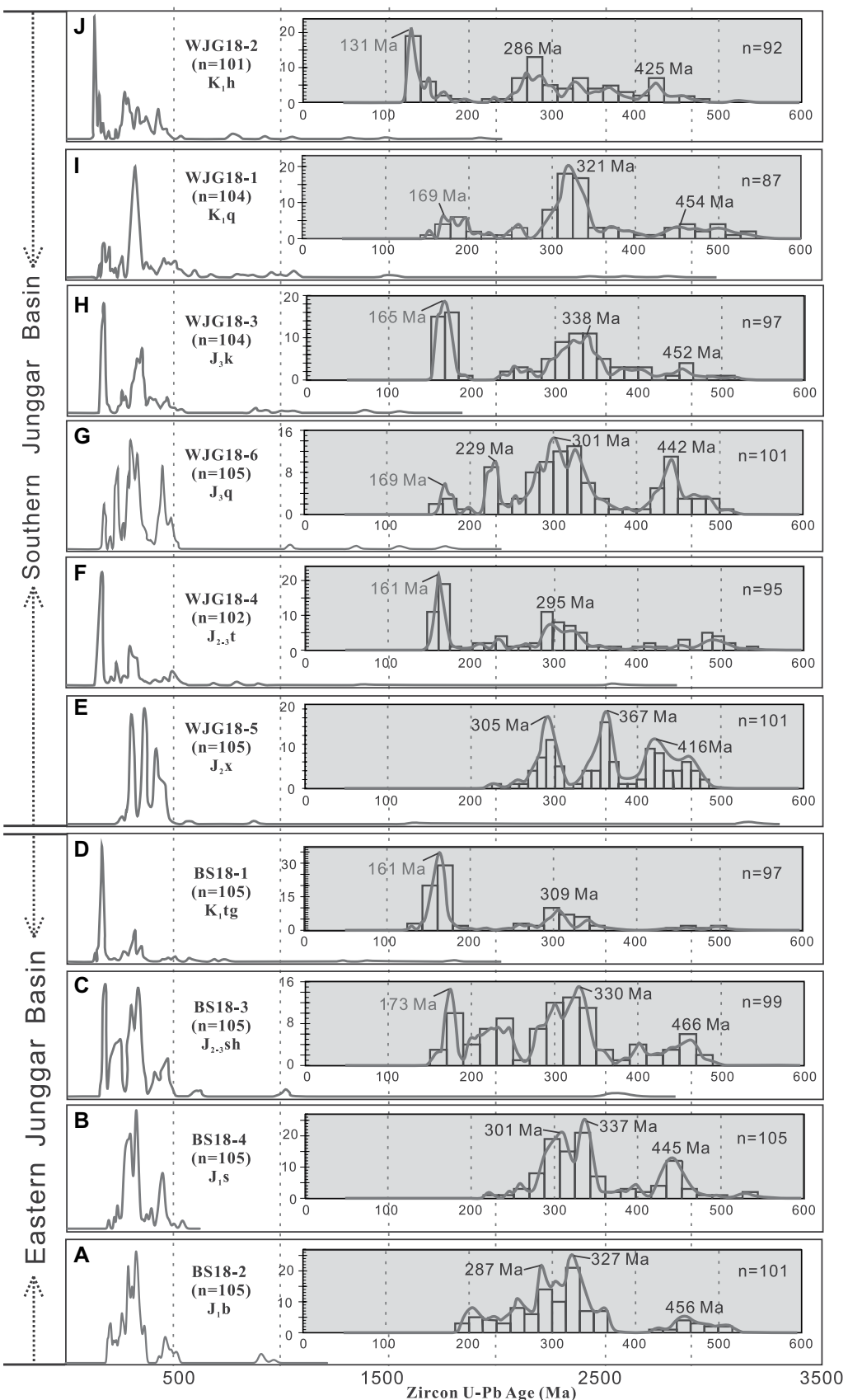


**Figure 8.** Relative probability plots and histograms (insets) show U-Pb ages of detrital zircons from the Lower Jurassic to Lower Cretaceous samples in (A–D) the eastern Junggar Basin and (E–J) the southern Junggar Basin.

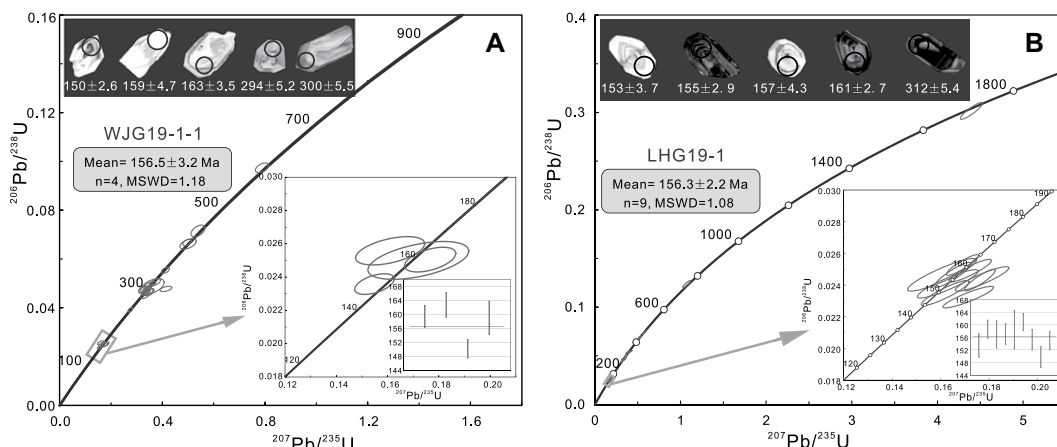


**Figure 9. Zircon U-Pb Concordia diagrams, cathodoluminescence (CL) images, and weighted mean  $^{206}\text{Pb}/^{238}\text{U}$  ages are shown for (A) gravels and (B) tuff samples.**

### Provenance Changes of the Southern Junggar Basin

The zircon U-Pb age spectrum of the Middle Jurassic Xishanyao Formation (sample WJG18-5) shows that there might have been a mixed provenance from the Yili-Central Tianshan Block and North Tianshan Arc (Fig. 10B). Specifically, it includes the late Carboniferous (peak at 367 Ma) to Early Permian (peak at 305 Ma) magmatic rocks of the North Tianshan Arc Block and the northern margin of the Yili-Central Tianshan Block, the Late Devonian magmatic rocks (peak at 416 Ma) of the Yili-Central Tianshan Block, and a few basement rocks (Fig. 8E). Fang et al. (2015) observed a few chert fragments in the Xishanyao Formation, which may come from the South Tianshan Belt. The increased contribution from the South Tianshan Belt and Yili-Central Tianshan Block implies that the topography of the North Tianshan Arc was probably smooth enough so that rivers could cut through and bring sediments from the South Tianshan Belt and Yili-Central Tianshan Block to the north during this period (Yang et al., 2013). In addition, meandering fluvial to lacustrine, coal-bearing deposits are well-developed inside the North Tianshan Arc (Fang et al., 2005), which indicates a low relief topography in the Middle Jurassic.

Compared with the Xishanyao Formation, the U-Pb ages from the detrital zircons of the Toutunhe Formation (sample WJG18-4) present an abrupt change with the first appearance of abundant Late Jurassic magmatic zircons (age peak of 161 Ma), which indicates a new source. These zircons were formed simultaneously during the deposition of the Toutunhe Formation, which suggests syn-depositional magmatism was occurring at this time (Fig. 10C). Fang et al. (2015) considered the Jurassic magmatic rocks of the northern Tianshan area to have been distributed initially along the North Tianshan Fault. The other source of zircons corresponds to the

late Paleozoic, post-collisional magmatic belt of the North Tianshan Arc (age peak of 295 Ma). Although Yang et al. (2013) suggested that a vast drainage system encompassed the North Tianshan Arc and Yili-Central Tianshan Block, the local recycling from the early Mesozoic cover also might have occurred in the late Middle Jurassic.

The Upper Jurassic Qigu Formation (sample WJG18-6) shows that the proportion of the Paleozoic age population rose markedly (Fig. 8G), which indicates that the sedimentary contribution of the Paleozoic magmatic rocks from the Tianshan Range further increased. In the Upper Jurassic Kalazha Formations (sample WJG18-3), the Middle–Late Jurassic zircons (peak age at 165 Ma) are dominant groups and attest to recycling from the Middle–Late Jurassic magmatic zircons underlying sedimentary strata in the North Tianshan Arc (Fig. 10D). The other two sources of zircons in the Kalazha Formation show some similarities to the Qigu Formation and again correspond to the late Paleozoic magmatic belt (peak age at 338 Ma) of the North Tianshan Arc and the early Paleozoic magmatic rocks (peak age at 452 Ma) of the Yili-Central Tianshan Block. This evidence suggests that the uplift and the subsequent erosional events started during the depositional period of the Toutunhe Formation rather than the Kalazha Formation. The older age groups may originate from zircons from the Proterozoic basement of the Yili-Central Tianshan Block.

The age spectrum of the Lower Cretaceous Qingshuihe Formation (sample WJG18-1) shows a dominant provenance from the late Carboniferous magmatic belt (peak age at 321 Ma) of the North Tianshan Arc (Fig. 10E). Fang et al. (2019) deemed that these sediments might also have been derived from the western Tianshan Volcanic Arc and older recycled sedimentary strata following the uplift of the Western Tianshan at the end of the Jurassic. The presence of

Jurassic magmatic zircons attests to recycling from the underlying sediments. The age spectrum of the Lower Cretaceous Hutubi Formation (sample WJG18-2) exhibits a dramatic change with the first appearance of zircons from contemporaneous Early Cretaceous magmatic sources (peak age at 131 Ma) (Fig. 8J), which indicates continuous magmatic activity throughout the southern Junggar Basin since the Middle Jurassic (Fig. 10E). We deduce that the sedimentary sources of the Hutubi Formation that contains Early Cretaceous detrital zircons were derived from the western Bogda Range (see discussion below). In addition, the increase in Late Silurian zircons (peak age at 425 Ma) demonstrates that the southern edge of the Junggar Basin extended to the south, and the Yili-Central Tianshan Block began to provide detritus again (Fig. 10E).

### Eastern versus Southern Junggar Basin

The age population patterns of the detrital zircons from the late Mesozoic sediments in the eastern and southern Junggar Basin exhibit apparent similarities. They are characterized by a significant multimodal distribution with dominant Paleozoic peak ages with minor Precambrian or late Mesozoic zircon populations, which indicates mixed magmatic sources. In addition, since the deposition of the Toutunhe Formation in the southern Junggar Basin and the Shishugou Formation in the eastern Junggar Basin, the provenance had experienced an abrupt change, with the first appearance of late Mesozoic magmatic sources. However, abundant Early Cretaceous zircons occur in the Lower Cretaceous Tugulu Group in the southern Junggar Basin rather than in the eastern Junggar. Considering that these zircons also did not appear in the Qingshuihe Formation in the southern Junggar Basin, we hypothesize that the Early Cretaceous magmatic rocks may have provided the main detritus for the upper part of the Lower Cretaceous sequences. Based on the detrital zircon

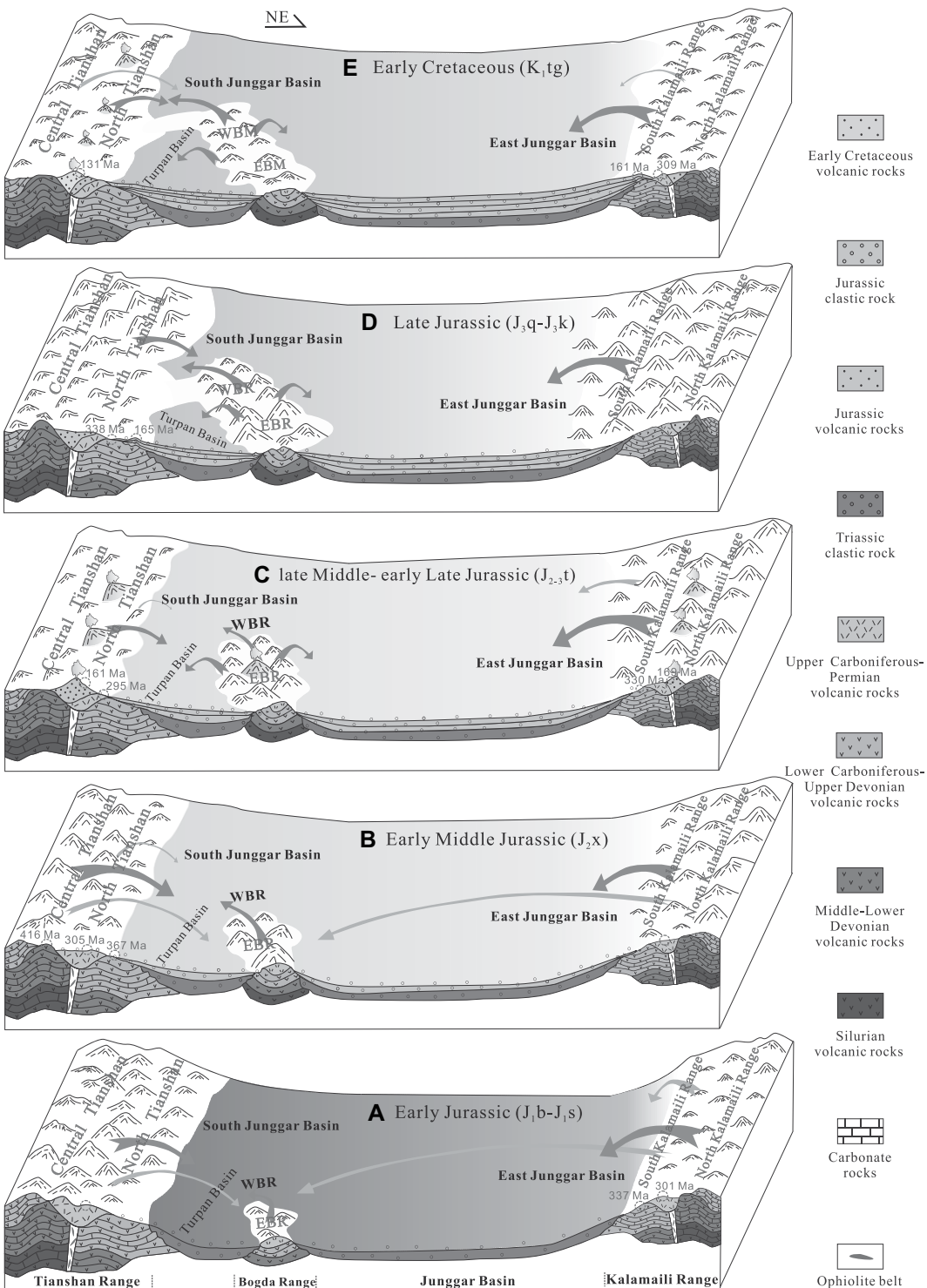


**Figure 10.** Paleogeographic and provenance evolution in the Tianshan Range and its adjacent areas during the Early Jurassic to Early Cretaceous. (A) During the Early Jurassic, the North Tianshan Arc was exhumed and provided detrital sediments to the southern Junggar Basin, while the Kalamaili and eastern Bogda Range were initially uplifted. (B) During the early Middle Jurassic, most parts of the Tianshan Range experienced continuous erosion and peneplanation, sedimentary sources of the southern Junggar Basin changed to the Yili-Central Tianshan Block, while the Kalamaili and eastern Bogda Ranges continued to uplift. (C) Volcanism occurred in the North Tianshan Arc and Kalamaili during the late Middle Jurassic. (D) During the Late Jurassic, the western (Chinese) Tianshan, Kalamaili, and Bogda Ranges experienced mutual uplift, and the sediments were mainly sourced from recycling of the underlying sedimentary strata. (E) The Tianshan (including the Bogda) and Kalamaili Ranges were eroded and exhumed during the Early Cretaceous. The dominant sources, minor sources, and lakes are indicated by thick arrows, thin arrows, and shaded areas, respectively. WBR—Western Bogda Range; EBR—Eastern Bogda Range.

geochronological data obtained in this study, sedimentary characteristics, and published data, we identify four tectonic evolution stages of the Tianshan-Kalamaili Ranges and Junggar Basin system from the Early Jurassic to the Early Cretaceous:

Stage 1: During the Early–Middle Jurassic period (ca. 201.3–166.2 Ma) (Figs. 10A–10B),

a large area of the Tianshan Range experienced continuous erosion and peneplanation processes, and the sediment sources of the southern Junggar Basin gradually changed from the late Paleozoic magmatic rocks of the North Tianshan Arc (Fig. 10A; Yang et al., 2013; Fang et al., 2015) to the more distal and older rocks (Precambrian and early Paleozoic) of the Yili-Central Tianshan

Block (Fig. 10B). However, the Kalamaili Range experienced episodic uplifts in this same period (Figs. 10A–10B). The late Paleozoic magmatic rock from the South Kalamaili Range provided primary sources for the eastern Junggar Basin. At the same time, the eastern Bogda Range also was subjected to episodic uplifts (Ji et al., 2019), whereas the western Bogda area

was a depositional region and received detrital materials from the latter mountain range (Fang et al., 2019; Ji et al., 2019). In addition, both northward and southward paleocurrents in Middle to Lower Jurassic sequences in the western Bogda area indicate that the North Tianshan Arc and Kalamaili Range were other vital source areas (Fang et al., 2019). The episodic uplifts of the Bogda Range are similar to the basin-range evolution between the Kalamaili Range and the eastern Junggar Basin (Ji et al., 2018, 2019, 2020; Fang et al., 2019), which implies that this episodic tectonism has a similar geo-dynamic origin.

Stage 2: By the time the Middle Jurassic Toutunhe Formation was deposited (ca. 166.2–160.8 Ma), the Tianshan Range formed a peneplanation surface, and syn-depositional magmatic rocks of the North Tianshan Arc supplied the dominant materials for the southern Junggar Basin (Fig. 10C). However, the Kalamaili Range and the eastern Bogda Range experienced distinct tectonic uplift during the deposition of the Toutunhe Formation that was accompanied by contemporaneous magmatic activity (Ji et al., 2018, 2020). They provided the detrital sediments for the eastern Junggar Basin and the western Bogda region.

Stage 3: The western Tianshan, Bogda, and Kalamaili Ranges subsequently experienced uplift during the deposition of the Late Jurassic Qigu and Kalazha Formations (ca. 160.8–145 Ma), whereas the peneplanation surface in other areas of the eastern Tianshan Range was preserved (Fig. 10D; Fang et al., 2019). The initial topographic disparity between the western and eastern Tianshan Range formed at this time (Ji et al., 2018). This Late Jurassic uplift in the western Tianshan (Dumitru et al., 2001; Wang et al., 2018b) and Bogda Ranges (Shen et al., 2006; Tang et al., 2015) was also recorded by apatite fission-track data.

Stage 4: During the Early Cretaceous, the Tianshan and Kalamaili Ranges experienced rapid exhumation and lake transgression was

initiated in the Junggar Basin. The detrital sediments were sourced primarily from the recycling of older sediments with the addition of an Early Cretaceous magmatic source (Fig. 10E). Also, plentiful late Mesozoic magmatic zircons occurred in detrital sediments, which indicates episodic magmatic activity throughout the southeastern Junggar Basin since the deposition of the Toutunhe Formation.

### Late Mesozoic Magmatic Activity in the Tianshan and Adjacent Areas

Compared with the samples of the Badaowan to Xishanyao Formations (ca. 201.3–166.2 Ma), a noticeable change in the age population pattern is the presence of plentiful Jurassic zircons with a peak age of 161 Ma in the Toutunhe Formation (sample WJG18-4) and the Shishugou Formation (sample BS18-3) (Fig. 11A). Generally, major episodes of magmatism in the Tianshan and adjacent areas occurred in the Paleozoic and locally extended to the Triassic (Guo et al., 2010). But since the late Mesozoic, the Tianshan has been an intracontinental region without widespread magmatism (Guo et al., 2010). However, in recent years, a growing number of field outcrops of late Mesozoic intrusions and volcanic rocks have been reported in the western (Xu et al., 2008), eastern (Pu et al., 1994; Vincent and Allen, 2001), and southern Junggar Ranges (Wang and Gao, 2012; Deng et al., 2010, 2015) and in the Bogda (Liu et al., 2019) and Altai Ranges (Liu et al., 2018).

Moreover, recent detrital zircon geochronological data and provenance analyses from the Meso-Cenozoic sediments in the southeastern Junggar Basin have revealed abundant late Mesozoic magmatic zircons in clastic sediments (Yang et al., 2013; Tang et al., 2014; Fang et al., 2015, 2019; Ji et al., 2018, 2020; Xiang et al., 2019). For example, Yang et al. (2013) found abundant Jurassic detrital zircons with a peak age of 168 Ma in the Toutunhe Formation in the Manasi River section, southern Junggar Basin.

Fang et al. (2015) suggested that the Toutunhe Formation is the earliest deposit that contains plentiful Late Jurassic magmatic zircons with a peak age of 157 Ma in the Toutunhe Formation section (southern Junggar Basin). Ji et al. (2018) and Fang et al. (2019) also found a noticeable change in age population patterns in the Toutunhe Formation in the Bogda Range compared with the underlying strata, with the occurrence of significant amounts of Middle–Late Jurassic zircons with peak ages of 165 Ma and 156 Ma. The Meso-Cenozoic detrital zircon data from the southeastern Junggar Basin areas obtained in previous studies also show the dominance of Middle–Late Jurassic zircons (with a peak age at 156 Ma) (Fig. 11B). These zircon clusters are elongated euhedral crystals with clear oscillatory zonation and high Th/U ratios, which is indicative of a magmatic origin. This evidence indicates that magmatic activity occurred in the Tianshan during the deposition of the Toutunhe Formation. However, previous studies have suggested that late Mesozoic magmatism was limited in volume (Yang et al., 2013) and broadly distributed along major strike-slip faults or rift belts in the Tianshan Range and adjacent areas (Guo et al., 2010). These Middle–Late Jurassic zircon ages also occur in the Upper Jurassic to Lower Cretaceous strata, which indicates that these late Mesozoic magmatic rocks continued to supply detrital material to the Junggar Basin.

Near the Honggou section in the Manas River valley, southern Junggar Basin, thin tuff layers have been reported in the lower part of the Qigu Formation (XBGMR, 1993), and the dated zircons yielded ages between ca. 164.4 Ma and ca. 156.9 Ma (Wang and Gao, 2012; Deng et al., 2015). This is relatively reliable evidence of late Mesozoic volcanic activity in the northern part of the Tianshan Range. Pu et al. (1994) also reported Late Jurassic tuffs in the lower part of the Qigu Formation in the Kalamaili and Bogda areas. In this contribution, a thin tuff layer is also reported from the lower part of the Qigu Formation (Figs. 4G and

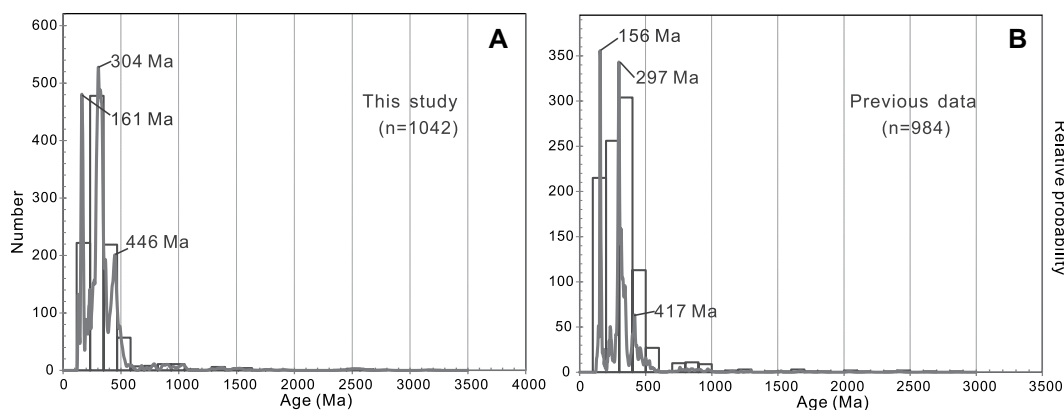


**Figure 11.** Combined relative probability density and histogram plots of (A) the samples from this study and (B) previous studies from the southeastern Junggar Basin are shown. Data in (B) are from Yang et al. (2013); Fang et al. (2015, 2019); and Ji et al. (2018).

4K) near Urumqi, which yielded a weighted mean zircon  $^{206}\text{Pb}/^{238}\text{U}$  age of  $156.3 \pm 2.2$  Ma (Fig. 9B). We also collected tuffaceous gravel samples (Fig. 4I) from the Lower Cretaceous Qingshuime Formation conglomerate (Fig. 4H) in the Wangjiagou section, and a weighted mean zircon  $^{206}\text{Pb}/^{238}\text{U}$  age of  $156.5 \pm 3.2$  Ma was obtained (Fig. 9A). These data show the same chronological characteristics as the tuff strata in the Honggou section of the Manasi River. Further, the formation age of the aforementioned tuff is identical within error to those of detrital magmatic zircons from the overlying strata. They thus may represent the source for the overlying strata. However, it is challenging to provide such a large amount of Mesozoic magmatic zircons for the overlying strata from only a few thin tuff layers because the tuff itself does not contain substantial magmatic zircons (Deng et al., 2015). Moreover, the Upper Qigu Formation could not represent the source of the underlying Toutunhe Formation.

Through 1:50,000 scale geological mapping, late Mesozoic magmatic rocks have been identified in the Tianshan and Junggar Ranges. For example, Liu et al. (2018) discovered several Early Jurassic trachyandesites in the Fuyun region. They obtained a zircon  $^{206}\text{Pb}/^{238}\text{U}$  age of  $181.9 \pm 0.7$  Ma, which confirms Early Jurassic magmatic activity in the northeastern Junggar Range. Liu et al. (2019) also found Late Jurassic monzonitic granite and diorite for the first time in the Mulei section of the Bogda Range. Zircon crystallization ages of  $154.9 \pm 1.9$  Ma and  $152.7 \pm 1.8$  Ma from these plutonic rocks were interpreted as their emplacement ages, which further provides evidence for Late Jurassic magmatic activity in the Tianshan Range. Also, from the Bogda Range, our group recently discovered an Early Cretaceous granodiorite outcrop with a crystallization age of  $131.9 \pm 1.5$  Ma (W.B., Zhu, 2021, personal commun.). In addition, a large number of Early Cretaceous detrital zircons with a peak age of 131 Ma were found in the Lower Cretaceous Hutubi Formation (K<sub>1</sub>h) of the southern Junggar Basin (Fig. 8J). Based on the southwestward paleocurrents in the study area (Fang et al., 2005), we deduce that the sedimentary sources of the Hutubi Formation, which contain the Early Cretaceous detrital zircons, might be derived from the western Bogda Range. These together provide solid evidence for Early Cretaceous magmatic activity in the Tianshan Range. Nevertheless, future investigations will be needed to better document the Jurassic–Early Cretaceous magmatism in the Tianshan, and this study provides insights from a sedimentological perspective.

## Dynamics of the Late Mesozoic Tectono-Magmatic Events

Hendrix et al. (1992) suggested that the late Mesozoic multi-stage uplift and related sedimentation in the Tianshan Range were correlated with three collisional events at the southern margin of Eurasia that include the collisions of the Qiangtang Block in the Late Triassic, the Lhasa Block in the latest Jurassic–earliest Cretaceous, and the Kohistan-Dras Arc in the Late Cretaceous. However, Vincent and Allen (2001) pointed out that the Early–Middle Jurassic strata in the eastern Junggar Basin contain numerous unconformities that do not match these collisional/accretionary events. For example, the unconformity at the base of the Middle Jurassic Xishanyao and Toutunhe Formations occurred between the time-gap of the Qiangtang-Kunlun accretion and the Lhasa-Qiangtang collision.

Unconformities at the base of the Lower Jurassic Badaowan and Sangonghe Formations and contemporaneous reverse faults were found localized in the Junggar Basin (Hendrix et al., 1992; Vincent and Allen, 2001; Yang et al., 2015a). Seismic profiles in the Junggar Basin show that pre-Jurassic strata underwent intense folding before the deposition of Jurassic strata, which formed a major angular unconformity at the base of the Lower Jurassic Badaowan Formation (Fig. 5). In addition, Yang et al. (2015a) suggested that the Late Triassic–Early Jurassic compressional deformation in Central Asia weakened northward. These unconformities were possibly related to the collision of the Qiangtang Block with Eurasia during the Late Triassic–Early Jurassic (Fig. 3; Glorie et al., 2010; De Grave et al., 2011; Jepson et al., 2018).

The disconformity at the base of the Middle Jurassic Xishanyao Formation is traceable in the central Junggar Basin and its eastern uplift (Vincent and Allen, 2001). Seismic profiles also show a basin-wide angular unconformity between the Lower Jurassic Sangonghe and Middle Jurassic Xishanyao Formations in the Turfan Basin (Greene et al., 2001). Yang et al. (2015a) proposed that this deformation was possibly related to the Early–Middle Jurassic closure of the western Mongol-Okhotsk Ocean (Fig. 3; Zorin, 1999). In addition, our detrital zircon U-Pb analyses show that the Yili-Central Tianshan Block provided detritus for the southern Junggar Basin during the deposition of the Badaowan-Xishanyao Formations (Figs. 10A–10B). Therefore, we hypothesize that the Tianshan Range was characterized by intense erosion during the Early–Middle Jurassic.

The unconformity between the Toutunhe and Xishanyao Formations is ubiquitous along the margins of the Junggar Basin (Figs. 4–5) and in

the Hoxtolgay Basin (Yang et al., 2015a). This study also suggests that during the deposition of the Toutunhe Formation, the Kalamaili and eastern Bogda Ranges were subjected to distinct tectonic uplift accompanied by contemporaneous magmatic activity, which provided the source materials of the sediment supply for the eastern Junggar Basin and western Bogda. These lines of evidence suggest that the eastern Junggar experienced an intense intraplate deformation with volcanism during the Middle–Late Jurassic (Yang et al., 2015a). The occurrence of the thick alluvial conglomerate of the Upper Jurassic Kalazha Formation along the margins of the Junggar also supports this point. Although the geodynamic origin of this tectonism is unclear, it might have resulted from the collision of the western Karakoram-Lhasa Block with Asia during the late Middle–Late Jurassic (Yang et al., 2017).

During the latest Jurassic–earliest Cretaceous, significant deformation such as folding occurred in the eastern Junggar Basin and completely changed the Late Jurassic structural and depositional pattern (Yang et al., 2015a, 2015b, 2017). The change of the sedimentary facies from the Upper Jurassic alluvial fan into the Lower Cretaceous lacustrine environment, together with the increased input of early Paleozoic detrital zircons, provide evidence for lake transgression and rapid uplift during this period (Fang et al., 2015). It is noted that the possible climate change (e.g., humid environment) in the Mesozoic could have triggered chemical weathering and led to enhanced surface erosion. However, angular unconformity surfaces along the Junggar Basin margins are well exposed in the field, which indicates that the underlying strata were strongly deformed. We hence prefer a tectonic origin for the widespread late Mesozoic unconformity in the study area. More importantly, coeval accelerated basement cooling in the western Chinese Tianshan (Wang et al., 2018b), Kyrgyzstan Tianshan (Jepson et al., 2018), and Bogda-Harlik Range (Zhu et al., 2006; Tang et al., 2015; Gillespie et al., 2017; Chen et al., 2020; He et al., 2022) was also recorded by low-temperature thermochronology. Our field observations, new sedimentological data, and seismic profiles solidly document this late Mesozoic episode of intracontinental deformation. It can be linked with significant compressional deformation driven by the contemporaneous accretion of the Kolyma-Omolon Block to the Siberian Craton (Oxman, 2003); closure of the Mongol-Okhotsk Ocean (Yang et al., 2015b); collision of the Karakoram-Lhasa Block to Eurasia (Yang et al., 2017); or the subduction of the Meso-Tethys oceanic plate (He et al., 2022). In addition, based on the zircon U-Pb ages of tuffs in the

lower part of the Upper Jurassic Qigu Formation and biostratigraphic evidence from the southeastern Junggar Basin, the initiation of the late Mesozoic tectono-magmatic event in the Tianshan Range and adjacent areas is constrained to have occurred in the late Middle Jurassic (ca. 160 Ma). This event was also probably related to the superimposed effect of the aforementioned tectonic episodes, which are generally regarded as major plate convergence sites in Central and East Asia during the late Mesozoic (Dong et al., 2000, 2007, 2015; Zhu et al., 2020).

## CONCLUSIONS

(1) Based on field observations and seismic profile analyses, several unconformity surfaces within the Middle to Late Jurassic strata of the Tianshan and Junggar Ranges were identified, which indicates late Mesozoic tectonic activity.

(2) Detrital zircon U-Pb dating results for the Lower Jurassic to Lower Cretaceous sandstones in the eastern and southern Junggar Basin, combined with published paleocurrent analyses, reveal a complex intracontinental tectonic evolution.

(3) Since the late Middle Jurassic, plentiful late Mesozoic magmatic zircons appear in the age spectra of the detrital samples, with peaks at ca. 161 Ma and ca. 131 Ma. Moreover, tuffaceous gravels and tuff samples yielded weighted mean zircon  $^{206}\text{Pb}/^{238}\text{U}$  ages of  $156.5 \pm 3.2$  Ma and  $156.3 \pm 2.2$  Ma, respectively, which indicates the presence of contemporary magmatic activity.

(4) Multi-directional tectonic deformation and multiple magmatic events occurred in the Tianshan Range and adjacent areas during the Jurassic and Early Cretaceous. They were possibly related to the superimposed effects induced by late Mesozoic multi-plate convergence in East Asia.

## ACKNOWLEDGMENTS

We thank two anonymous reviewers for detailed and constructive comments and associate editor Yongjiang Liu for editorial handling. This study was supported by the National Key R&D Plan of China (grants 2017YFC0601402 and 2018YFC0603703). The support provided by the China Scholarship Council (CSC, 201806190214) is appreciated for financing the research stay of Z. He in Belgium. We thank Rongsong Tian and Hailin Wu for generating diagrams. We are also grateful to Technician Bin Wu at the State Key Laboratory for Mineral Deposits Research, Nanjing University, China, for his help with zircon geochronology analyses.

## REFERENCES CITED

- Allen, M.B., Windley, B.F., and Zhang, C., 1993, Palaeozoic collisional tectonics and magmatism of the Chinese Tien Shan, Central Asia: *Tectonophysics*, v. 220, p. 89–115, [https://doi.org/10.1016/0040-1951\(93\)90225-9](https://doi.org/10.1016/0040-1951(93)90225-9).
- Avouac, J.P., Tapponnier, P., Bai, M., You, H., and Wang, G., 1993, Active thrusting and folding along the northern Tien Shan and late Cenozoic rotation of the Tarim relative to Dzungaria and Kazakhstan: *Journal of Geophysical Research: Solid Earth*, v. 98, p. 6755–6804, <https://doi.org/10.1029/92JB01963>.
- Bian, W.H., Hornung, J., Liu, Z.H., Wang, P.J., and Hindler, M., 2010, Sedimentary and palaeoenvironmental evolution of the Junggar Basin, Xinjiang, Northwest China: Palaeobiodiversity and Palaeoenvironments, v. 90, p. 175–186, <https://doi.org/10.1007/s12549-010-0038-9>.
- Charreau, J., Gumiaux, C., Avouac, J.P., Augier, R., Chen, Y., Barrier, L., and Wang, Q., 2009, The Neogene Xiyu Formation, diachronous prograding gravel wedge at front of the Tianshan: Climatic and tectonic implications: *Earth and Planetary Science Letters*, v. 287, p. 298–310, <https://doi.org/10.1016/j.epsl.2009.07.035>.
- Charvet, J., Shu, L.S., and Laurent-Charvet, S., 2007, Palaeozoic structural and geodynamic evolution of eastern Tianshan (NW China): Welding of the Tarim and Junggar plates: *Episodes Journal of International Geoscience*, v. 30, p. 162–186.
- Charvet, J., Shu, L., Laurent-Charvet, S., Wang, B., Faure, M., Cluzel, D., and De Jong, K., 2011, Palaeozoic tectonic evolution of the Tianshan belt, NW China: *Science China Earth Sciences*, v. 54, p. 166–184, <https://doi.org/10.1007/s11430-010-4138-1>.
- Chen, K., Gumiaux, C., Augier, R., Chen, Y., Wang, Q.C., Lin, W., and Wang, S.L., 2011, The Mesozoic palaeorelief of the northern Tianshan (China): *Terra Nova*, v. 23, p. 195–205, <https://doi.org/10.1111/j.1365-3121.2011.00999.x>.
- Chen, K., Lin, W., and Wang, Q.C., 2015, The Bogeda Shan uplifting: Evidence from multiple phases of deformation: *Journal of Asian Earth Sciences*, v. 99, p. 1–12, <https://doi.org/10.1016/j.jseaes.2014.12.006>.
- Chen, X., Lu, H.F., Shu, L.S., Wang, H.M., and Zhang, G.Q., 2002, Study on tectonic evolution of Junggar Basin [in Chinese with English abstract]: *Geological Journal of China Universities*, v. 8, p. 257–267.
- Chen, X., Shu, L.S., Santosh, M., and Zhao, X.X., 2013, Island arc-type bimodal magmatism in the eastern Tianshan Belt, Northwest China: *Geochemistry, zircon U-Pb geochronology and implications for the Paleozoic crustal evolution in Central Asia: Lithos*, v. 168, p. 48–66, <https://doi.org/10.1016/j.lithos.2012.10.006>.
- Chen, Y., Wang, G.C., Kapp, P., Shen, T.Y., Zhang, P., Zhu, C.Y., and Cao, K., 2020, Episodic exhumation and related tectonic controlling during Mesozoic in the Eastern Tian Shan, Xinjiang, northwestern China: *Tectonophysics*, v. 796, <https://doi.org/10.1016/j.tecto.2020.228647>.
- Corfu, F., Hanchar, J.M., Hoskin, P.W., and Kinny, P., 2003, Atlas of zircon textures: Reviews in mineralogy and geochemistry, v. 53, p. 469–500, <https://doi.org/10.2113/0530469>.
- De Grave, J., Buslov, M.M., and Van Den Haute, P., 2007, Distant effects of India-Eurasia convergence and Mesozoic intracontinental deformation in Central Asia: Constraints from apatite fission-track thermochronology: *Journal of Asian Earth Sciences*, v. 29, p. 188–204, <https://doi.org/10.1016/j.jseaes.2006.03.001>.
- De Grave, J., Glorie, S., Buslov, M.M., Izmer, A., Fournier-Carrie, A., Batalev, V.Y., Vanhaecke, F., Elburg, M.A., and Van den Haute, P., 2011, The thermo-tectonic history of the Song-Kul Plateau, Kyrgyz Tien Shan: Constraints by apatite and titanite thermochronometry and zircon U/Pb dating: *Gondwana Research*, v. 20, p. 745–763, <https://doi.org/10.1016/j.gr.2011.03.011>.
- De Grave, J., Glorie, S., Buslov, M.M., Stockli, D.F., McWilliams, M.O., Batalev, V. Yu, and Van den Haute, P., 2013, Thermo-tectonic history of the Issyk-Kul basement (Kyrgyz northern Tien Shan, Central Asia): *Gondwana Research*, v. 23, p. 998–1020, <https://doi.org/10.1016/j.gr.2012.06.014>.
- De Pelsmaeker, E., Jolivet, M., Laborde, A., Poujol, M., Robin, C., Zhimulev, F.I., Nachtergaelie, S., Glorie, S.,
- De Clercq, S., Batalev, V.Y., and De Grave, J., 2018, Source-to-sink dynamics in the Kyrgyz Tien Shan from the Jurassic to the Paleogene: Insights from sedimentological and detrital zircon U-Pb analyses: *Gondwana Research*, v. 54, p. 180–204, <https://doi.org/10.1016/j.gr.2017.09.004>.
- Deng, S.H., Lu, Y.Z., Fan, R., Pan, Y.H., and Fang, L.H., 2010, The Jurassic System of Northern Xinjiang, China [in Chinese]: Hefei, Anhui, China, University of Science & Technology of China Press, p. 279.
- Deng, S.H., Wang, S.E., Yang, Z.Y., Lu, Y.Z., Li, X., Hu, Q.Y., An, C.Z., Xi, D.P., and Wan, X.J., 2015, Comprehensive study of the Middle–Upper Jurassic strata in the Junggar Basin, Xinjiang [in Chinese with English abstract]: *Acta Geoscientica Sinica*, v. 36, p. 559–574.
- Dong, S.W., Wu, X.H., Wu, Z.H., Deng, J.F., Gao, R., and Wang, C.S., 2000, On tectonic seesawing of the East Asia continent—Global implication of the Yanshanian movement [in Chinese with English abstract]: *Geological Review*, v. 46, p. 8–13.
- Dong, S.W., Zhang, Y.Q., Long, C.X., Yang, Z.Y., Ji, Q., Wang, T., Hu, J.M., and Chen, X.H., 2007, Jurassic tectonic revolution in China and new interpretation of the Yanshan Movement [in Chinese with English abstract]: *Acta Geologica Sinica*, v. 81, p. 1449–1461.
- Dong, S.W., Zhang, Y.Q., Zhang, F.Q., Cui, J.J., Chen, X.H., Zhang, S.H., Miao, L.C., Li, J.H., Shi, W., Li, Z.H., Huang, S.Q., and Li, H.L., 2015, Late Jurassic–Early Cretaceous continental convergence and intracontinental orogenesis in East Asia: A synthesis of the Yanshan Revolution: *Journal of Asian Earth Sciences*, v. 114, p. 750–770, <https://doi.org/10.1016/j.jseaes.2015.08.011>.
- Dong, Y.P., Zhang, G.W., Neubauer, F., Liu, X.M., and Hauzenberger, C., 2011, Syn- and post-collisional granitoids in the Central Tianshan Orogen: Geochemistry, geochronology and implications for tectonic evolution: *Gondwana Research*, v. 20, p. 568–581, <https://doi.org/10.1016/j.gr.2011.01.013>.
- Dumitru, T.A., Zhou, D., Chang, E.Z., Graham, S.A., Hendrix, M.S., Sobel, E.R., and Davis, G.A., 2001, Uplift, exhumation, and deformation in the Chinese Tianshan: *Geological Society of America*, v. 194, p. 71–100.
- Fang, S.H., Guo, Z.J., Song, Y., Wu, C.D., Zhang, Z.C., Wang, M.N., and Fan, R.D., 2005, Sedimentary facies evolution and basin pattern of the Jurassic in southern margin area of Junggar Basin [in Chinese with English abstract]: *Journal of Palaeogeography*, v. 7, p. 347–356.
- Fang, S.H., Guo, Z.J., Wu, C.D., Zhang, Z.C., Wang, M.N., and Yuan, Q.D., 2006, Jurassic clastic composition in the southern Junggar Basin, Northwest China: Implications for basin-range pattern and tectonic attributes [in Chinese with English abstract]: *Acta Geologica Sinica*, v. 80, p. 196–209.
- Fang, Y.N., Wu, C.D., Guo, Z.J., Hou, K.J., Dong, L., Wang, L.X., and Li, L.L., 2015, Provenance of the southern Junggar Basin in the Jurassic: Evidence from detrital zircon geochronology and depositional environments: *Sedimentary Geology*, v. 315, p. 47–63, <https://doi.org/10.1016/j.sedgeo.2014.10.014>.
- Fang, Y.N., Wu, C.D., Wang, Y.Z., Wang, L., Guo, Z.J., and Hu, H., 2016, Stratigraphic and sedimentary characteristics of the Upper Jurassic–Lower Cretaceous strata in the Junggar Basin, Central Asia: Tectonic and climate implications: *Journal of Asian Earth Sciences*, v. 129, p. 294–308, <https://doi.org/10.1016/j.jseaes.2016.09.001>.
- Fang, Y.N., Wu, C.D., Wang, Y.Z., Hou, K.L., and Guo, Z.J., 2019, Topographic evolution of the Tianshan Range and their relation to the Junggar and Turpan Basins, Central Asia, from the Permian to the Neogene: *Gondwana Research*, v. 75, p. 47–67, <https://doi.org/10.1016/j.gr.2019.03.020>.
- Gao, J., Li, M.S., Xiao, X.C., Tang, Y.Q., and He, G.Q., 1998, Paleozoic tectonic evolution of the Tianshan Orogen, northwestern China: *Tectonophysics*, v. 287, p. 213–231, [https://doi.org/10.1016/S0040-1951\(97\)00211-4](https://doi.org/10.1016/S0040-1951(97)00211-4).
- Gao, J., Long, L.L., Klemd, R., Qian, Q., Liu, D.Y., Xiong, X.M., Su, W., Liu, W., Wang, Y.T., and Yang, F.Q., 2009, Tectonic evolution of the South Tianshan orogen and adjacent regions, NW China: Geochemical and age constraints of granitoid rocks: *International Journal of Earth Sciences*, v. 98, p. 1221–1238, <https://doi.org/10.1007/s00531-008-0370-8>.

- Gillespie, J., Glorie, S., Jepson, G., Zhang, Z.Y., Xiao, W.J., Danišk, M., and Collins, A.S., 2017, Differential exhumation and crustal tilting in the easternmost Tianshan (Xinjiang, China), revealed by low-temperature thermochronology: *Tectonics*, v. 36, p. 2142–2158, <https://doi.org/10.1002/2017TC004574>.
- Glorie, S., De Grave, J., Buslov, M.M., Elburg, M.A., Stockli, D.F., Gerdes, A., and Van den Haute, P., 2010, Multi-method chronometric constraints on the evolution of the Northern Kyrgyz Tien Shan granitoids (Central Asian Orogenic Belt): From emplacement to exhumation: *Journal of Asian Earth Sciences*, v. 38, p. 131–146, <https://doi.org/10.1016/j.jseaes.2009.12.009>.
- Glorie, S., De Grave, J., Buslov, M.M., Zhimulev, F.I., Stockli, D.F., Batalev, V.Y., and Izmer, A., 2011, Tectonic history of the Kyrgyz South Tien Shan (Atbashi-Inylchek) suture zone: The role of inherited structures during deformation-propagation: *Tectonics*, v. 30, TC6016, <https://doi.org/10.1029/2011TC002949>.
- Greene, T.J., Carroll, A.R., Hendrix, M.S., Graham, S.A., Wartes, M.A., and Abbink, O.A., 2001, Sedimentary record of Mesozoic deformation and inception of the Turpan–Hamí basin, north-west China: *Geological Society of America Bulletin*, v. 194, p. 317–340.
- Guo, Z.J., Wu, C.D., Zhang, Z.C., Wang, M.N., and Fang, S.H., 2005, Mesozoic–Cenozoic relationships between Tianshan Mountain and peripheral basins: Evidences from sedimentology and exhumation of Jurassic in Houxia area, Urumchi [in Chinese with English abstract]: *Geological Journal of China Universities*, v. 11, p. 558–567.
- Guo, Z.J., Han, B.F., Zhang, Y.Y., and Chen, S., 2010, Mesozoic and Cenozoic crust–mantle interaction in the Central Asian Orogenic Belt: A comparative study of mantle-derived magmatic rocks in northern Xinjiang [in Chinese with English abstract]: *Acta Petrologica Sinica*, v. 26, p. 431–439.
- Han, B.F., Guo, Z.J., Zhang, Z.C., Zheng, L., Chen, J.F., and Song, B., 2010, Age, geochemistry, and tectonic implications of a late Paleozoic stitching pluton in the North Tianshan suture zone, western China: *Geological Society of America Bulletin*, v. 122, p. 627–640, <https://doi.org/10.1130/B26491.1>.
- Han, B.F., He, G.Q., Wang, X.C., and Guo, Z.J., 2011, Late Carboniferous collision between the Tarim and Kazakhstan–Yili terranes in the western segment of the South Tianshan Orogen, Central Asia, and implications for the Northern Xinjiang, western China: *Earth-Science Reviews*, v. 109, p. 74–93, <https://doi.org/10.1016/j.earscirev.2011.09.001>.
- Han, Y.G., and Zhao, G.C., 2018, Final amalgamation of the Tianshan and Junggar orogenic collage in the southwestern Central Asian Orogenic Belt: Constraints on the closure of the Paleo-Asian Ocean: *Earth-Science Reviews*, v. 186, p. 129–152, <https://doi.org/10.1016/j.earscirev.2017.09.012>.
- Han, Y.G., Zhao, G.C., Sun, M., Eizenhöfer, P.R., Hou, W.Z., Zhang, X.R., and Wang, B., 2016a, Detrital zircon provenance constraints on the initial uplift and denudation of the Chinese western Tianshan after the assembly of the southwestern Central Asian Orogenic Belt: *Sedimentary Geology*, v. 339, p. 1–12, <https://doi.org/10.1016/j.sedgeo.2016.03.028>.
- Han, Y.G., Zhao, G.C., Sun, M., Eizenhöfer, P.R., Hou, W.Z., Zhang, X.R., Liu, Q., Wang, B., Liu, D.X., and Xu, B., 2016b, Late Paleozoic subduction and collision processes during the amalgamation of the Central Asian Orogenic Belt along the South Tianshan suture zone: *Lithos*, v. 246, p. 1–12, <https://doi.org/10.1016/j.lithos.2015.12.016>.
- He, D.F., Zhou, L., Tang, Y., Wu, X.Z., and Du, S.G., 2007, Characteristics of unconformity between the Xishanya Formation and Toutunhe Formation of Middle Jurassic in Junggar Basin and its significance in petroleum exploration [in Chinese with English abstract]: *Journal of Palaeogeography*, v. 9, p. 387–396.
- He, Z.Y., Wang, B., Zhong, L.L., and Zhu, X.Y., 2018, Crustal evolution of the Central Tianshan Block: Insights from zircon U-Pb isotopic and structural data from meta-sedimentary and meta-igneous rocks along the Wulasitai–Wulanmoren shear zone: *Precambrian Research*, v. 314, p. 111–128, <https://doi.org/10.1016/j.precamres.2018.06.003>.
- He, Z.Y., Wang, B., Nachtergaelie, S., Glorie, S., Ni, X.H., Su, W.B., Cai, D.X., Liu, J.S., and De Grave, J., 2021a, Long-term topographic evolution of the Central Tianshan (NW China) constrained by low-temperature thermochronology: *Tectonophysics*, v. 817, <https://doi.org/10.1016/j.tecto.2021.229066>.
- He, Z.Y., Wang, B., Ni, X.H., De Grave, J., Scaillet, S., Chen, Y., Liu, J.S., and Zhu, X., 2021b, Structural and kinematic evolution of strike-slip shear zones around and in the Central Tianshan: Insights for eastward tectonic wedging in the southwest Central Asian Orogenic Belt: *Journal of Structural Geology*, v. 144, <https://doi.org/10.1016/j.jsg.2021.104279>.
- He, Z.Y., Wang, B., Glorie, S., Su, W.B., Ni, X.H., Jepson, G., Liu, J.S., Zhong, L.L., Gillespie, J., and De Grave, J., 2022, Mesozoic building of the Eastern Tianshan and Junggar (NW China) revealed by low-temperature thermochronology: *Gondwana Research*, v. 103, p. 37–53, <https://doi.org/10.1016/j.gr.2021.11.013>.
- Hendrix, M.S., 2000, Evolution of Mesozoic sandstone compositions, Southern Junggar, northern Tarim, and western Turpan basins, northwest China: A detrital record of the ancestral Tianshan: *Journal of Sedimentary Research*, v. 70, p. 520–532, <https://doi.org/10.1306/2DC40924-E047-11D7-8643000102C1865D>.
- Hendrix, M.S., Graham, S.A., Carroll, A.R., Sober, E.R., McKnight, C.L., Shulein, B.J., and Wang, Z.X., 1992, Sedimentary record and climatic implications of recurrent deformation of the Tien Shan: Evidence from Mesozoic strata of the North Tarim, South Junggar and Turpan basins: *Geological Society of America Bulletin*, v. 104, p. 53–79, [https://doi.org/10.1130/0016-7606\(1992\)104<0053:SRACIO>2.3.CO;2](https://doi.org/10.1130/0016-7606(1992)104<0053:SRACIO>2.3.CO;2).
- Hendrix, M.S., Dumitru, T.A., and Graham, S.A., 1994, Late Oligocene–Early Miocene unroofing in the Chinese Tien Shan: An early effect of the India-Asia collision: *Geology*, v. 22, p. 487–490, [https://doi.org/10.1130/0091-7613\(1994\)022<0487:LOEMUI>2.3.CO;2](https://doi.org/10.1130/0091-7613(1994)022<0487:LOEMUI>2.3.CO;2).
- Hoskin, P.W.O., and Black, L.P., 2000, Metamorphic zircon formation by solid-state recrystallization of protolith igneous zircon: *Journal of Metamorphic Geology*, v. 18, p. 423–439, <https://doi.org/10.1046/j.1525-1314.2000.00266.x>.
- Huang, G., Niu, G.Z., Wang, X.L., Guo, J., and Yu, F., 2012, Formation and emplacement age of Karamaili ophiolite: LA-ICP-MS zircon U-Pb age evidence from the diabase and tuff in eastern Junggar, Xinjiang [in Chinese with English abstract]: *Geological Bulletin of China*, v. 31, p. 1267–1278.
- Huang, H., Zhang, Z.C., Santosh, M., Zhang, D.Y., Zhao, Z.D., and Liu, J.L., 2013, Early Paleozoic tectonic evolution of the South Tianshan Collisional Belt: Evidence from geochemistry and zircon U-Pb geochronology of the Tieke Monzonite Pluton, Northwest China: *The Journal of Geology*, v. 121, p. 401–424, <https://doi.org/10.1086/670653>.
- Jepson, G., Glorie, S., Konopelko, D., Gillespie, J., Danisik, M., Mirkalov, R., Mamadjanov, Y., and Collins, A.S., 2018, Low-temperature thermochronology of the Chatkal-Kurama terrane (Uzbekistan-Tajikistan): Insights into the Meso-Cenozoic thermal history of the western Tian Shan: *Tectonics*, v. 37, p. 3954–3969, <https://doi.org/10.1029/2017TC004878>.
- Ji, H.J., Tao, H.F., Wang, Q., Qiu, Z., Ma, D.X., Qiu, J.L., and Liao, P., 2018, Early to Middle Jurassic tectonic evolution of the Bogda mountains, Northwest China: Evidence from sedimentology and detrital zircon geochronology: *Journal of Asian Earth Sciences*, v. 153, p. 57–74, <https://doi.org/10.1016/j.jseaes.2017.03.018>.
- Ji, H.J., Tao, H.F., Wang, Q., Ma, D.X., and Hao, L.W., 2019, Petrography, geochemistry, and geochronology of Lower Jurassic sedimentary rocks from the Northern Tianshan (West Bogda area), Northwest China: Implications for provenance and tectonic evolution: *Geological Journal*, v. 54, p. 1688–1714, <https://doi.org/10.1002/gj.3263>.
- Ji, H.J., Tao, H.F., Qiu, J.L., and Wei, H.Y., 2020, Provenance of Middle Jurassic clastic rocks from the Bogda area of Eastern Tianshan and its implications: *International Geology Review*, v. 62, p. 1319–1342, <https://doi.org/10.1080/00206814.2019.1647119>.
- Jolivet, M., Dominguez, S., Charreau, J., Chen, Y., Li, Y., and Wang, Q., 2010, Mesozoic and Cenozoic tectonic history of the central Chinese Tianshan: Reactivated tectonic structures and active deformation: *Tectonics*, v. 29, TC6019, <https://doi.org/10.1029/2010TC002712>.
- Jolivet, M., Heilbronn, G., Robin, C., Barrier, L., Bourquin, S., Guo, Z.J., Jia, Y., Guerit, L., Yang, W., and Fu, B., 2013, Reconstructing the Late Paleozoic–Mesozoic topographic evolution of the Chinese Tianshan: Available data and remaining uncertainties: *Advances in Geosciences*, v. 37, p. 7–18, <https://doi.org/10.5194/ageo-37-7-2013>.
- Konopelko, D., Seltmann, R., Biske, G., Lepekhina, E., and Sergeev, S., 2009, Possible source dichotomy of contemporaneous post-collisional barren I-type versus tin-bearing A-type granites, lying on opposite sides of the South Tien Shan suture: *Ore Geology Reviews*, v. 35, p. 206–216, <https://doi.org/10.1016/j.oregeorev.2009.01.002>.
- Kröner, A., Kovach, V., Belousova, E., Hegner, E., Armstrong, R., Dolgopolova, A., and Rytsk, E., 2014, Reassessment of continental growth during the accretionary history of the Central Asian Orogenic Belt: *Gondwana Research*, v. 25, p. 103–125, <https://doi.org/10.1016/j.gr.2012.12.023>.
- Li, C.X., Guo, Z.J., and Dupont-Nivet, G., 2011, Late Cenozoic tectonic deformation across the northern foreland of the Chinese Tianshan: *Journal of Asian Earth Sciences*, v. 42, p. 1066–1073, <https://doi.org/10.1016/j.jseaes.2010.08.009>.
- Li, J.Y., Yang, T.N., Li, Y.P., and Zhu, Z.X., 2009, Geological features of the Karamaili faulting belt, eastern Junggar region, Xinjiang, China and its constraints on the reconstruction of Late Paleozoic ocean-continent framework of the Central Asian region [in Chinese with English abstract]: *Geological Bulletin of China*, v. 28, p. 1817–1826.
- Li, Z.H., Chen, G., Cui, J.B., Chen, Z.J., He, J.Y., Ding, C., and Yang, F., 2014, Fission-track age of Yanbian tectonic-thermal events in the northern Junggar Basin [in Chinese with English abstract]: *Geological Science and Technology Information*, v. 33, p. 9–14.
- Liu, S.B., Dou, H., Zhang, W.M., Peng, Z.J., Zhang, L., and Zhang, W.R., 2018, Discovery of Jurassic trachyanidesite and its geological significance in the northwestern of Junggar Basin [in Chinese with English abstract]: *Geological Review*, v. 64, p. 1519–1529.
- Liu, S.B., Dou, H., Li, H.B., and Wen, Z.G., 2019, Geological significance of the discovery of Late Jurassic intermediate-acidic intrusive rock in Bogeda area of East Tianshan, Xinjiang, and its U-Pb zircon age [in Chinese with English abstract]: *Geological Bulletin of China*, v. 38, p. 288–294.
- Long, X.P., Yuan, C., Sun, M., Safonova, I., Xiao, W.J., and Wang, Y.J., 2012, Geochemistry and U-Pb detrital zircon dating of Paleozoic graywackes in East Junggar, NW China: insights into subduction-accretion processes in the southern Central Asian Orogenic Belt: *Gondwana Research*, v. 21, p. 637–653, <https://doi.org/10.1016/j.gr.2011.05.015>.
- Ma, X.X., Shu, L.S., Meert, J.G., and Li, J.Y., 2014, The Paleozoic evolution of Central Tianshan: Geochemical and geochronological evidence: *Gondwana Research*, v. 25, p. 797–819, <https://doi.org/10.1016/j.gr.2013.05.015>.
- Molnar, P., and Tapponier, P., 1975, Cenozoic tectonics of Asia: Effects of a continental collision: *Science*, v. 189, p. 419–426, <https://doi.org/10.1126/science.189.4201.419>.
- Nachtergaelie, S., De Pelsmaeker, E., Glorie, S., Zhitulev, F., Jolivet, M., Danišk, M., Buslov, M.M., and De Grave, J., 2018, Meso-Cenozoic tectonic evolution of the Talaq-Fergana region of the Kyrgyz Tien Shan revealed by low-temperature basement and detrital thermochronology: *Geoscience Frontiers*, v. 9, p. 1495–1514, <https://doi.org/10.1016/j.gsf.2017.11.007>.
- Oxman, V.S., 2003, Tectonic evolution of the Mesozoic Verkhoyansk-Kolyma belt (NE Asia): *Tectonophysics*, v. 365, p. 45–76, [https://doi.org/10.1016/S0040-1951\(03\)00064-7](https://doi.org/10.1016/S0040-1951(03)00064-7).
- Pu, R.H., Mei, Z.C., and Tang, Z.H., 1994, Division of seismic sequences and interpretation on sequence

- stratigraphy of Shishugou Group, Cainan Area [in Chinese with English abstract]: *Earth Science*, v. 19, p. 769–777.
- Sengör, A.M.C., Natal'In, B.A., and Burtman, V.S., 1993, Evolution of the Altaiid tectonic collage and Palaeozoic crustal growth in Eurasia: *Nature*, v. 364, p. 299–307, <https://doi.org/10.1038/364299a0>.
- Shen, C.B., Mei, L.F., Liu, L., Tang, J.G., and Zhou, F., 2006, Evidence from apatite and zircon fission track analysis for Mesozoic–Cenozoic uplift thermal history of Bogda Mountain of Xinjiang, Northwest China [in Chinese with English abstract]: *Marine Geology & Quaternary Geology*, v. 26, p. 87–92.
- Su, W.B., Cai, K.D., Sun, M., Wang, X.S., Bao, Z.H., He, Z.Y., and De Grave, J., 2021, Carboniferous back-arc extension in the southern Yili-Central Tianshan Block and its significance to the formation of the Kazakhstan Orogen: Insights from the Wusun Mountain volcanic belt: *International Journal of Earth Sciences*, <https://doi.org/10.1007/s00531-021-02111-y>.
- Tang, W.H., Zhang, Z.C., Li, J.F., Li, K., Chen, Y., and Guo, Z.J., 2014, Late Paleozoic to Jurassic tectonic evolution of the Bogda area (northwest China): Evidence from detrital zircon U-Pb geochronology: *Tectonophysics*, v. 626, p. 144–156, <https://doi.org/10.1016/j.tecto.2014.04.005>.
- Tang, W.H., Zhang, Z.C., Li, J.F., Li, K., Luo, Z., and Chen, Y., 2015, Mesozoic and Cenozoic uplift and exhumation of the Bogda Mountain, NW China: Evidence from apatite fission track analysis: *Geoscience Frontiers*, v. 6, p. 617–625, <https://doi.org/10.1016/j.gsf.2014.04.006>.
- Vincent, S.J., and Allen, M.B., 2001, Sedimentary record of Mesozoic intracontinental deformation in the eastern Junggar Basin, northwest China: Response to orogeny at the Asian margin, in Hendrix, M.S., and Davis, G.A., eds., *Paleozoic and Mesozoic Tectonic Evolution of Central Asia—From Continental Assembly to Intracontinental Deformation*: Geological Society of America Memoir, v. 194, p. 341–360, <https://doi.org/10.1130/0-8137-1194-0.341>.
- Wang, B., Faure, M., Cluzel, D., Shu, L.S., Charvet, J., Meffre, S., and Ma, Q., 2006, Late Paleozoic tectonic evolution of the northern West Chinese Tianshan Belt: *Geodinamica Acta*, v. 19, p. 237–247, <https://doi.org/10.3166/ga.19.237-247>.
- Wang, B., Liu, H., Shu, L., Jahn, B.M., Chung, S.L., Zhai, Y., and Liu, D., 2014, Early Neoproterozoic crustal evolution in northern Yili Block: Insights from migmatite, orthogneiss and leucogranite of the Wenquan metamorphic complex in the NW Chinese Tianshan: *Precambrian Research*, v. 242, p. 58–81, <https://doi.org/10.1016/j.precamres.2013.12.006>.
- Wang, S.E., and Gao, L.Z., 2012, SHRIMP U-Pb dating of zircons from tuff of Jurassic Qigu Formation in Junggar Basin, Xinjiang [in Chinese with English abstract]: *Geological Bulletin of China*, v. 31, p. 503–509.
- Wang, X.S., Gao, J., Klemd, R., Jiang, T., Li, J.L., Zhang, X., and Xue, S.C., 2017, The central Tianshan Block: A microcontinent with a Neoarchean Paleoproterozoic basement in the southwestern Central Asian Orogenic Belt: *Precambrian Research*, v. 295, p. 130–150, <https://doi.org/10.1016/j.precamres.2017.03.030>.
- Wang, Y.J., Jia, D., Pan, J.G., Wei, D.T., Tang, Y., Wang, G.D., Wei, C.R., and Ma, D.L., 2018a, Multiple-phase tectonic superposition and reworking in the Junggar Basin of northwestern China—Implications for deep-seated petroleum exploration: *American Association of Petroleum Geologists Bulletin*, v. 102, p. 1489–1521, <https://doi.org/10.1306/10181716518>.
- Wang, Y.N., Cai, K.D., Sun, M., Xiao, W.J., Grave, J.D., Wan, B., and Bao, Z.H., 2018b, Tracking the multi-stage exhumation history of the western Chinese Tianshan by apatite fission track (AFT) dating: Implication for the preservation of epithermal deposits in the ancient orogen belt: *Ore Geology Reviews*, v. 100, p. 111–132, <https://doi.org/10.1016/j.oregeorev.2017.04.011>.
- Wartes, M.A., Carroll, A.R., and Greene, T.J., 2002, Permian sedimentary record of the Turpan-Hami basin and adjacent regions, northwest China: Constraints on post-magmatic tectonic evolution: *Geological Society of America Bulletin*, v. 114, p. 131–152, [https://doi.org/10.1130/0016-7606\(2002\)114<0131:PSROTT>2.0.CO;2](https://doi.org/10.1130/0016-7606(2002)114<0131:PSROTT>2.0.CO;2).
- Windley, B.F., Alexeev, D., Xiao, W., Kröner, A., and Bardach, G., 2007, Tectonic models for accretion of the Central Asian Orogenic Belt: *Journal of the Geological Society*, v. 164, p. 31–47, <https://doi.org/10.1144/0016-76492006-022>.
- XBGMR (Xinjiang Bureau of Geology and Mineral Resources), 1965, Regional geological map of Kalamaili Shan sheet (L-45-30) [in Chinese]: Xinjiang Bureau of Geology and Mineral Resources, scale 1:200,000.
- XBGMR (Xinjiang Bureau of Geology and Mineral Resources), 1993, Regional geology of Xinjiang Uygur Autonomy Region [in Chinese]: Beijing, Geology Publishing House, 841 p.
- XBGMR (Xinjiang Bureau of Geology and Mineral Resources), 2007, Regional geologic map of Tianshan and adjacent area [in Chinese]: Beijing, Geological Publishing House, scale 1:1000,000.
- Xiang, D.F., Zhang, Z.Y., Xiao, W.J., Zhu, W.B., Zheng, D.W., Li, G.W., Zheng, B.H., Song, D.F., Han, C.M., and Pang, J.Z., 2019, Episodic Meso-Cenozoic denudation of Chinese Tianshan: Evidence from detrital apatite fission track and zircon U-Pb data, southern Junggar Basin margin, NW China: *Journal of Asian Earth Sciences*, v. 175, p. 199–212, <https://doi.org/10.1016/j.jseaea.2018.07.042>.
- Xiao, W.J., Zhang, L.C., Qin, K.Z., Sun, S., and Li, J.L., 2004, Paleozoic accretionary and collisional tectonics of the eastern Tianshan (China): Implications for the continental growth of Central Asia: *American Journal of Science*, v. 304, p. 370–395, <https://doi.org/10.2475/ajs.304.4.370>.
- Xiao, W.J., Windley, B.F., Yan, Q.R., Qin, K.Z., Chen, H.L., Yuan, C., Sun, M., Li, J.L., and Sun, S., 2006, SHRIMP zircon age of the Aermantai ophiolite in the North Xinjiang area, China and its tectonic implications (in Chinese with English abstract): *Acta Geologica Sinica*, v. 80, p. 32–37.
- Xiao, W.J., Han, C.M., Yuan, C., Sun, M., Lin, S.F., Chen, H.L., Li, Z.L., Li, J.L., and Sun, S., 2008, Middle Cambrian to Permian subduction related accretionary orogenesis of Northern Xinjiang, NW China: Implications for the tectonic evolution of Central Asia: *Journal of Asian Earth Sciences*, v. 32, p. 102–117, <https://doi.org/10.1016/j.jseaea.2007.10.008>.
- Xiao, W.J., Windley, B.F., Yuan, C., Sun, M., Han, C.M., and Lin, S.F., 2009, Paleozoic multiple subduction accretion processes of the southern Altaiids: *American Journal of Science*, v. 309, p. 221–270, <https://doi.org/10.2475/03.2009.02>.
- Xu, X., Chen, C., Ding, T.F., Liu, X.Y., and Li, H.Q., 2008, Discovery of Lisa basalt northwestern edge of Junggar Basin and its geological significance [in Chinese with English abstract]: *Xinjiang Geology*, v. 26, p. 9–16.
- Xiao, W.J., Han, C.M., Liu, W., Wan, B., Zhang, J.E., Ao, S.J., Zhang, Z.Y., Song, D.F., Tian, Z.H., and Luo, J., 2014, How many sutures in the southern Central Asian orogenic belt: Insights from east Xinjiang–west Gansu (NW China)?: *Geoscience Frontiers*, v. 5, p. 525–536, <https://doi.org/10.1016/j.gsf.2014.04.002>.
- Xu, X.W., Jiang, N., Li, X.H., Wu, C., Qu, X., Zhou, G., and Dong, L.H., 2015, Spatial temporal framework for the closure of the Junggar Ocean in Central Asia: New SIMS zircon U-Pb ages of the ophiolitic mélange and collisional igneous rocks in the Zhifang area, East Junggar: *Journal of Asian Earth Sciences*, v. 111, p. 470–491, <https://doi.org/10.1016/j.jseaea.2015.06.017>.
- Yang, W., Jolivet, M., Dupont-Nivet, G., Guo, Z., Zhang, Z., and Wu, C., 2013, Source to sink relations between the Tianshan and Junggar Basin (northwest China) from Late Palaeozoic to Quaternary: Evidence from detrital U-Pb zircon geochronology: *Basin Research*, v. 25, p. 219–240, <https://doi.org/10.1111/j.1365-2117.2012.00558.x>.
- Yang, Y.T., Song, C.C., and He, S., 2015a, Jurassic tectonostratigraphic evolution of the Junggar Basin, NW China: A record of Mesozoic intraplate deformation in Central Asia: *Tectonics*, v. 34, p. 86–115, <https://doi.org/10.1002/2014TC003640>.
- Yang, Y.T., Guo, Z.X., Song, C.C., Li, X.B., and He, S., 2015b, A short-lived but significant Mongol-Okhotsk collisional orogeny in latest Jurassic–earliest Cretaceous: *Gondwana Research*, v. 28, p. 1096–1116, <https://doi.org/10.1016/j.gr.2014.09.010>.
- Yang, Y.T., Guo, Z.X., and Luo, Y.J., 2017, Middle–Late Jurassic tectonostratigraphic evolution of Central Asia, implications for the collision of the Karakoram-Lhasa Block with Asia: *Earth-Science Reviews*, v. 166, p. 83–110, <https://doi.org/10.1016/j.earscirev.2017.01.005>.
- Yin, A., and Harrison, T.M., 2000, Geologic evolution of the Himalayan-Tibetan orogen: Annual Review of Earth and Planetary Sciences, v. 28, p. 211–280, <https://doi.org/10.1146/annurev.earth.28.1.211>.
- Zhang, A.Q., Afonso, J.C., Xu, Y.X., Wu, S.C., Yang, Y.J., and Yang, B., 2019, The deep lithospheric structure of the Junggar terrane, NW China: Implications for its origin and tectonic evolution: *Journal of Geophysical Research: Solid Earth*, v. 124, p. 11615–11638, <https://doi.org/10.1029/2019JB018302>.
- Zhao, Z.Y., Zhang, Z.C., Santosh, M., Huang, H., Cheng, Z.G., and Ye, J.C., 2015, Early Paleozoic magmatic record from the northern margin of the Tarim Craton: Further insights on the evolution of the Central Asian Orogenic Belt: *Gondwana Research*, v. 28, p. 328–347, <https://doi.org/10.1016/j.gr.2014.04.007>.
- Zhong, L.L., Wang, B., de Jong, K., Zhai, Y.Z., and Liu, H.S., 2019, Deformed continental arc sequences in the south Tianshan: New constraints on the early Paleozoic accretionary tectonics of the Central Asian Orogenic Belt: *Tectonophysics*, v. 768, <https://doi.org/10.1016/j.tecto.2019.228169>.
- Zhu, W.B., Shu, L.S., Sun, Y., Wang, F., and Zhao, Z.Y., 2006, Mesozoic–Cenozoic tectonic deformation of the central structure belt in Turpan-Hami basin, northwest China: Implications for the evolution of an intracontinental basin, Central Asia: *International Geology Review*, v. 48, p. 271–285, <https://doi.org/10.2747/0020-6814.48.3.271>.
- Zhu, W.B., Wang, F.J., Cao, Y.Y., and Wang, S.L., 2020, Tectono-magmatic events in Tianshan Range and adjacent areas during Yanshanian Movement period [in Chinese with English abstract]: *Acta Geologica Sinica*, v. 94, p. 1331–1346.
- Zhu, X.Y., Wang, B., Cluzel, D., He, Z.Y., Zhou, Y., and Zhong, L.L., 2019, Early Neoproterozoic gneissic granitoids in the southern Yili Block (NW China): constraints on microcontinent provenance and assembly in the SW Central Asian Orogenic Belt: *Precambrian Research*, v. 325, p. 111–131, <https://doi.org/10.1016/j.precamres.2019.02.019>.
- Zorin, Y.A., 1999, Geodynamics of the western part of the Mongolia-Okhotsk collisional belt, Trans-Baikal region (Russia) and Mongolia: *Tectonophysics*, v. 306, p. 33–56, [https://doi.org/10.1016/S0040-1951\(99\)00042-6](https://doi.org/10.1016/S0040-1951(99)00042-6).

SCIENCE EDITOR: WENJIAO XIAO  
ASSOCIATE EDITOR: YONGJIANG LIU

MANUSCRIPT RECEIVED 3 SEPTEMBER 2021  
REVISED MANUSCRIPT RECEIVED 16 NOVEMBER 2021  
MANUSCRIPT ACCEPTED 26 DECEMBER 2021

Printed in the USA